




# Analysis of 1,25-Dihydroxyvitamin D<sub>3</sub> Genomic Action Reveals Calcium-Regulating and Calcium-Independent Effects in Mouse Intestine and Human Enteroids

Shanshan Li,<sup>a</sup> Jessica De La Cruz,<sup>a</sup> Steven Hutchens,<sup>b</sup> Somshuvra Mukhopadhyay,<sup>b</sup> Zachary K. Criss,<sup>c</sup> Rohit Aita,<sup>d</sup> Oscar Pellon-Cardenas,<sup>d</sup> Joseph Hur,<sup>d</sup> Patricia Soteropoulos,<sup>a,e</sup> Seema Husain,<sup>a,e</sup> Puneet Dhawan,<sup>a,e</sup> Lieve Verlinden,<sup>f</sup> Geert Carmeliet,<sup>f</sup> James C. Fleet,<sup>g</sup> Noah F. Shroyer,<sup>c</sup> Michael P. Verzi,<sup>d</sup>  Sylvia Christakos<sup>a</sup>

<sup>a</sup>Department of Microbiology, Biochemistry and Molecular Genetics, Rutgers, The State University of New Jersey, New Jersey Medical School, Newark, New Jersey, USA

<sup>b</sup>Division of Pharmacology and Toxicology, College of Pharmacy, Institute for Cellular and Molecular Biology and Institute for Neuroscience, The University of Texas at Austin, Austin, Texas, USA

<sup>c</sup>Integrative Molecular and Biomedical Sciences Graduate Program, Division of Medicine, Baylor College of Medicine, Houston, Texas, USA

<sup>d</sup>Department of Genetics, Rutgers University, New Brunswick, New Jersey, USA

<sup>e</sup>Genomics Center, Rutgers, The State University of New Jersey, New Jersey Medical School, Newark, New Jersey, USA

<sup>f</sup>Laboratory of Clinical and Experimental Endocrinology, Department of Chronic Diseases and Metabolism, Leuven, Belgium

<sup>g</sup>Department of Nutrition Science, Purdue University, West Lafayette, Indiana, USA

**ABSTRACT** Although vitamin D is critical for the function of the intestine, most studies have focused on the duodenum. We show that transgenic expression of the vitamin D receptor (VDR) only in the distal intestine of VDR null mice (KO/TG mice) results in the normalization of serum calcium and rescue of rickets. Although it had been suggested that calcium transport in the distal intestine involves a paracellular process, we found that the 1,25-dihydroxyvitamin D<sub>3</sub> [1,25(OH)<sub>2</sub>D<sub>3</sub>]-activated genes in the proximal intestine associated with active calcium transport (*Trpv6*, *S100g*, and *Atp2b1*) are also induced by 1,25(OH)<sub>2</sub>D<sub>3</sub> in the distal intestine of KO/TG mice. In addition, *Slc30a10*, encoding a manganese efflux transporter, was one of the genes most induced by 1,25(OH)<sub>2</sub>D<sub>3</sub> in both proximal and distal intestine. Both villus and crypt were found to express *Vdr* and VDR target genes. RNA sequence (RNA-seq) analysis of human enteroids indicated that the effects of 1,25(OH)<sub>2</sub>D<sub>3</sub> observed in mice are conserved in humans. Using *Slc30a10*<sup>-/-</sup> mice, a loss of cortical bone and a marked decrease in *S100g* and *Trpv6* in the intestine was observed. Our findings suggest an interrelationship between vitamin D and intestinal Mn efflux and indicate the importance of distal intestinal segments to vitamin D action.

**KEYWORDS** calcium, manganese, transporters, intestine, vitamin D, human enteroids, mouse, *Slc30a10*, TRPV6

The essential role of vitamin D is to mediate calcium homeostasis through its regulatory effects on intestine, bone, and kidney (1). Vitamin D has also been reported to affect numerous other physiological processes not involved in calcium regulation, including immunomodulatory effects and inhibition of cancer progression (1). The skeletal and extraskeletal effects of 1,25-dihydroxyvitamin D<sub>3</sub> [1,25(OH)<sub>2</sub>D<sub>3</sub>] (the biologically active form of vitamin D [calcitriol]) are mediated by the vitamin D receptor (VDR), a nuclear protein which heterodimerizes with the retinoid X receptor (RXR). VDR/RXR interacts with DNA sequences and vitamin D response elements (VDREs) in target genes and leads to activation or repression of transcription. 1,25(OH)<sub>2</sub>D<sub>3</sub> also recruits coregulatory complexes that participate in the regulation of transcription of VDR target genes. VDR-mediated gene transcription is a multistep process requiring the

**Citation** Li S, De La Cruz J, Hutchens S, Mukhopadhyay S, Criss ZK, Aita R, Pellon-Cardenas O, Hur J, Soteropoulos P, Husain S, Dhawan P, Verlinden L, Carmeliet G, Fleet JC, Shroyer NF, Verzi MP, Christakos S. 2021. Analysis of 1,25-dihydroxyvitamin D<sub>3</sub> genomic action reveals calcium-regulating and calcium-independent effects in mouse intestine and human enteroids. *Mol Cell Biol* 41:e00372-20. <https://doi.org/10.1128/MCB.00372-20>.

**Copyright** © 2020 American Society for Microbiology. All Rights Reserved.

Address correspondence to Sylvia Christakos, [christak@njms.rutgers.edu](mailto:christak@njms.rutgers.edu).

**Received** 23 July 2020

**Returned for modification** 5 October 2020

**Accepted** 24 October 2020

**Accepted manuscript posted online** 2 November 2020

**Published** 21 December 2020

spatial and sequential combination of transcriptional coactivators and is influenced by the particular subcellular environment in a gene-specific manner (2, 3).

A principal target tissue of vitamin D action is the intestine (1, 4, 5). However, little is known about the molecular targets mediating the effects of vitamin D on intestinal biology. The classic role of  $1,25(\text{OH})_2\text{D}_3$  is the regulation of intestinal calcium absorption, which is crucial for bone health. When the need for calcium increases, for example, during periods of habitual low calcium intake and during growth, vitamin D-mediated intestinal calcium absorption occurs predominantly by an active transcellular process. The most pronounced effects of  $1,25(\text{OH})_2\text{D}_3$  during the active calcium transport process are increased synthesis of the epithelial calcium channel TRPV6 and the intracellular calcium binding protein calbindin- $\text{D}_{9k}$  (4, 5). In addition to the active transcellular pathway, calcium can also be absorbed via a nonsaturable paracellular process (4, 5). Whether  $1,25(\text{OH})_2\text{D}_3$  regulates calcium absorption by modulating genes associated solely with the facilitated diffusion model or whether  $1,25(\text{OH})_2\text{D}_3$  affects the paracellular process has been a matter of debate (6–9). Most research on calcium absorption has utilized the proximal small intestine, and early studies reported that  $1,25(\text{OH})_2\text{D}_3$ -regulated active calcium transport was localized only in the duodenum (9). It had been suggested that calcium absorption in the distal intestine reflects vitamin D-independent passive diffusion (10). However, previous studies also noted that  $1,25(\text{OH})_2\text{D}_3$  and low dietary calcium can regulate active calcium absorption in the distal intestines of rats (11–13). In addition, we recently showed that transgenic expression of VDR only in the distal intestine (distal ileum, cecum, and colon) at levels equivalent to those in wild-type (WT) mice results in normal calcium homeostasis and reverses the VDR-dependent rickets of the VDRnull mice (14). These findings indicate the importance of the distal intestinal segments to vitamin D action.

Although the classical intestinal role of  $1,25(\text{OH})_2\text{D}_3$  is the regulation of calcium absorption,  $1,25(\text{OH})_2\text{D}_3$  has been reported to have other important effects on the intestine, including the protection of the integrity of the mucosal barrier, regulation of pathogen invasion, apoptosis, nutrient transport, and cellular differentiation (7, 15–19). However, the molecular responses to  $1,25(\text{OH})_2\text{D}_3$  resulting in these effects in proximal versus those in distal intestine are poorly understood. In addition, although intestinal epithelial cells at the villi have been identified as targets for  $1,25(\text{OH})_2\text{D}_3$ , little is known about the effect of  $1,25(\text{OH})_2\text{D}_3$  in crypts; whether  $1,25(\text{OH})_2\text{D}_3$  responses occur in crypts has been a matter of debate (20–22). Thus, the diversity and complexity of vitamin D signaling in the intestine have not been fully clarified.

In this study, to further understand the role of vitamin D in the intestine, we examined the expression of VDR targets using transgenic mice with expression of VDR restricted to the distal intestine (KO/TG mice) (14) and compared our findings in these transgenic mice to vitamin D targets in both proximal and distal intestines of vitamin D-deficient mice treated with  $1,25(\text{OH})_2\text{D}_3$ . The classic  $1,25(\text{OH})_2\text{D}_3$ -activated genes found in the proximal intestine and associated with active calcium transport (*Trpv6*, *S100g*, and *Atp2b1*) were also induced in the distal intestine. In addition, one of the genes most induced by  $1,25(\text{OH})_2\text{D}_3$  in the proximal and distal intestine was *Slc30a10*, a manganese (Mn) efflux transporter which has recently been found to be critical for protection against neurotoxicity and liver injury which occur in the presence of elevated Mn levels (23). Both villus and crypts were found to express high levels of VDR and result in  $1,25(\text{OH})_2\text{D}_3$ -mediated target gene induction. RNA sequence (RNA-seq) analysis of human enteroids confirmed the induction of the same genes in mice and humans (*TRPV6*, *SLC30A10*, *ATP2B1*, and *CYP24A1*) in both villus and crypts, indicating, for the first time, direct transcriptomic responses to  $1,25(\text{OH})_2\text{D}_3$  in human enteroids in both crypt and villus-like compartments. Studies in *Slc30a10*<sup>-/-</sup> mice showed a loss of cortical bone and a marked decrease in *S100g* and *Trpv6* in the intestine of these mice. Our findings suggest that  $1,25(\text{OH})_2\text{D}_3$  may have a role not only to maintain calcium homeostasis but also in the cellular homeostasis of other divalent ions. Our findings emphasize the importance of the distal as well as the proximal intestine in order to

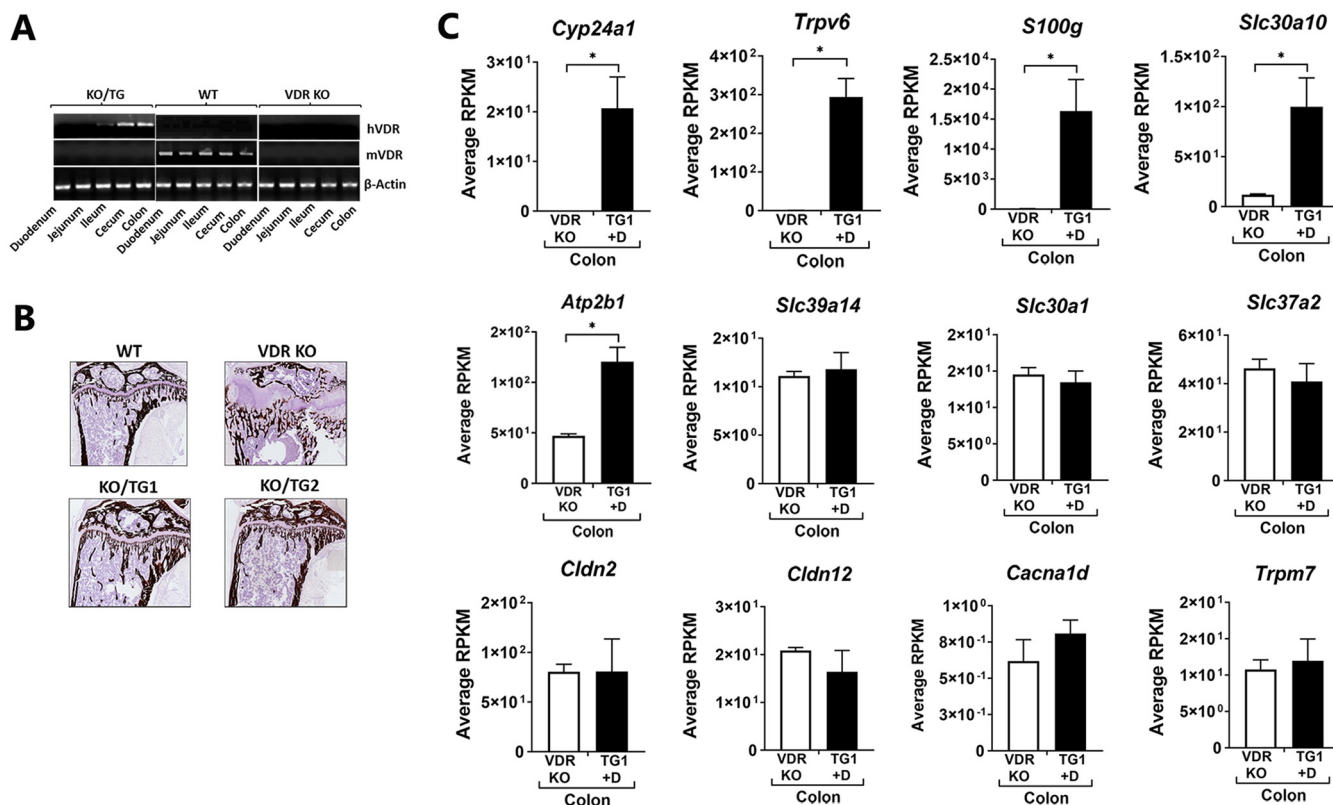


**FIG 1** Gene expression measured by RNA-seq in the colon of KO/TG1 mice treated with 1,25(OH)<sub>2</sub>D<sub>3</sub>. (A) KO/TG mice express VDR only in the distal intestine. Expression of hVDR is restricted to the distal intestines of KO/TG mice. Mouse (m) VDR is absent in KO/TG mice. (B) Rescue of VDR-dependent rickets in the KO/TG mice (Von Kossa staining [14]). (C) Gene expression in the colon of KO/TG mice treated with 1,25(OH)<sub>2</sub>D<sub>3</sub> (TG1 +D) compared to that in VDR KOs. Gene expression, measured by RNA-seq analysis, is shown as the mean of reads per kilobase per million (RPKM) ± SEM. *n* = 4 per group \*, *P* < 0.05.

understand intestinal effects of 1,25(OH)<sub>2</sub>D<sub>3</sub> and show that the effects of 1,25(OH)<sub>2</sub>D<sub>3</sub> involve intestinal epithelial cells in both villus and crypt.

## RESULTS

**RNA-seq analysis of transcriptomic responses to 1,25(OH)<sub>2</sub>D<sub>3</sub> in the colons of mice with transgenic expression of VDR only in the distal intestine.** Although most studies have focused on calcium absorption in the proximal intestine, our previous study demonstrated that transgenic expression of VDR only in the distal intestine rescued VDR-dependent rickets observed in the VDR knockout (KO) mouse (14). To understand mechanisms by which 1,25(OH)<sub>2</sub>D<sub>3</sub> acts to regulate intestinal biology not only in the proximal but also in the distal intestine, transcriptomic profiling was conducted to examine the expression of genes induced by 1,25(OH)<sub>2</sub>D<sub>3</sub> in the distal intestine of KO/TG mice (KO/TG line 1, noted as TG1), which express VDR exclusively in the distal intestine (distal ileum, cecum, and colon) (14) (Fig. 1A and B). We focused on the colon as a possible unappreciated target for regulation of calcium homeostasis. As noted in Fig. 1C the classic 1,25(OH)<sub>2</sub>D<sub>3</sub>-activated genes in the proximal intestine were also the genes most markedly induced by 1,25(OH)<sub>2</sub>D<sub>3</sub> in the colon of the TG mice (*Cyp24a1*, *Trpv6*, and *S100g*). Induction of *S100g* and *Trpv6* as well as *Atp2b*, genes involved in active calcium transport (1), suggests that active calcium transport in the distal intestine is involved in the normalization of mineral homeostasis in these mice. Genes associated with passive calcium transport, *Cldn2*, *Cldn12* or *Cacna1d* (Cav1.3 gene), and *Trpm7*, which have been suggested as channels other than *Trpv6* for the regulation of intestinal calcium absorption (6, 24, 25), were not significantly regulated by 1,25(OH)<sub>2</sub>D<sub>3</sub> in the colon. In addition to the classic 1,25(OH)<sub>2</sub>D<sub>3</sub>-activated genes, *Slc30a10*, the gene for a manganese efflux transporter located in the apical/luminal

domain, was also one of the genes most induced by  $1,25(\text{OH})_2\text{D}_3$  and was the principal *Slc* transporter gene affected by  $1,25(\text{OH})_2\text{D}_3$ . Other *Slc* transporter genes, including *Slc30a1* (a Zn transporter) as well as *Slc30a4* and *Slc30a5* (also Zn transporters [not shown]), *Slc39a14* (a Mn transporter which mediates Mn reuptake from the basolateral membrane), and *Slc37a2* (a phosphate-linked glucose 6 phosphate antiporter), were not significantly affected by  $1,25(\text{OH})_2\text{D}_3$ . Real-time PCR (RT-PCR) analysis of intestinal tissues from the same transgenic mouse line (KO/TG1) (Fig. 2A) as well as from a second independent KO/TG line (KO/TG2, noted as TG2) (Fig. 2B) validated the RNA-seq analyses, indicating that the genes most responsive to  $1,25(\text{OH})_2\text{D}_3$  in the distal intestine of KO/TG mice include *Cyp24a1*, *Trpv6*, *S100g*, and *Slc30a10*. Other *Slc* transporter genes, *Slc30a1* and *Slc37a2*, were unaffected by  $1,25(\text{OH})_2\text{D}_3$  (Fig. 2). Due to the expression of VDR only in the distal intestine, the duodenum of KO/TG mice was unresponsive to  $1,25(\text{OH})_2\text{D}_3$  (Fig. 2, Duo).

**Regulation of vitamin D target genes in the intestine.** In addition to the induction of *Slc30a10* in the distal intestine of transgenic mice, *Slc30a10* was found to be regulated by  $1,25(\text{OH})_2\text{D}_3$  in different intestinal segments (duodenum, ileum, and colon) of vitamin D-deficient mice similarly as other vitamin D target genes (*Cyp24a1* and *S100g*). *Slc37a2*, although not regulated by  $1,25(\text{OH})_2\text{D}_3$  in the distal intestine, was induced by  $1,25(\text{OH})_2\text{D}_3$  in the duodenum (Fig. 3). In addition, in the duodenum expression of *Slc30a4*, *Slc30a5*, *Slc39a14*, *Trmp7*, *Cldn12*, and *Cacna1d*, similar to findings in the colon (Fig. 1), was unaffected by  $1,25(\text{OH})_2\text{D}_3$  treatment of vitamin D-deficient mice ( $n = 4$ ; vehicle versus  $1,25(\text{OH})_2\text{D}_3$  treated,  $P > 0.5$ ). *Cldn2*, however, was significantly induced by  $1,25(\text{OH})_2\text{D}_3$  in the duodenum of these mice (3.8-fold,  $n = 4$ ; vehicle versus  $1,25(\text{OH})_2\text{D}_3$  treated,  $P < 0.05$ ).

To gain insight into a possible role of vitamin D in the regulation of Mn transport, further studies were conducted comparing the regulation of *Slc30a10* in the intestine to the regulation of known vitamin D target genes. As shown in Fig. 4A, *Slc30a10* and *Trpv6* showed similar time courses of induction by  $1,25(\text{OH})_2\text{D}_3$ . Gene expression for these transporters was significantly induced in the duodenum at 4 h after injection and then decreased to control levels at 24 h after  $1,25(\text{OH})_2\text{D}_3$  administration. Similar findings were observed for *Slc30a10* and *Trpv6* in colon (data not shown). These findings suggest a rapid response of *Trpv6* and *Slc30a10* to  $1,25(\text{OH})_2\text{D}_3$  for intestinal calcium or Mn transport.

In addition to regulation by  $1,25(\text{OH})_2\text{D}_3$ , effects of dietary calcium on the expression of these genes was also examined. Four-week-old mice were fed either a high-calcium (1%) or low-calcium diet (0.02%) diet for 4 weeks. As shown in Fig. 4B, under conditions of low dietary calcium [which results in increased circulating  $1,25(\text{OH})_2\text{D}_3$  levels] (1) an induction in both *Slc30a10* and *Trpv6* was observed in the duodenum. A similar induction of these genes in response to low dietary calcium was also observed in the colon (not shown). *S100g* was also significantly increased in duodenum and colon in response to low dietary calcium (data not shown). These findings suggest coregulation of these manganese and calcium transporters under conditions of dietary calcium alteration.

In additional studies, developmental changes in the expression of *Slc30a10* and *Trpv6* were compared. *Trpv6* was not expressed significantly in the intestine until after birth and was induced at 3 weeks of age, the time of weaning in mice, which coincides with the increase in active intestinal calcium transport (Fig. 4C) (26). Unlike *Trpv6*, *Slc30a10* was detected in the fetal intestine. The most marked induction in the expression of *Slc30a10* in the intestine was observed between fetal samples and at 1 week postpartum. Thus, developmental changes in intestinal *Slc30a10* and *Trpv6* do not coincide, suggesting that different factors modulate the developmental expression of these transporters.

To further understand a possible interrelationship between vitamin D and manganese homeostasis, vitamin D target genes associated with  $1,25(\text{OH})_2\text{D}_3$ -mediated calcium transport were examined in the intestine of the *Slc30a10*<sup>-/-</sup> mice, which have

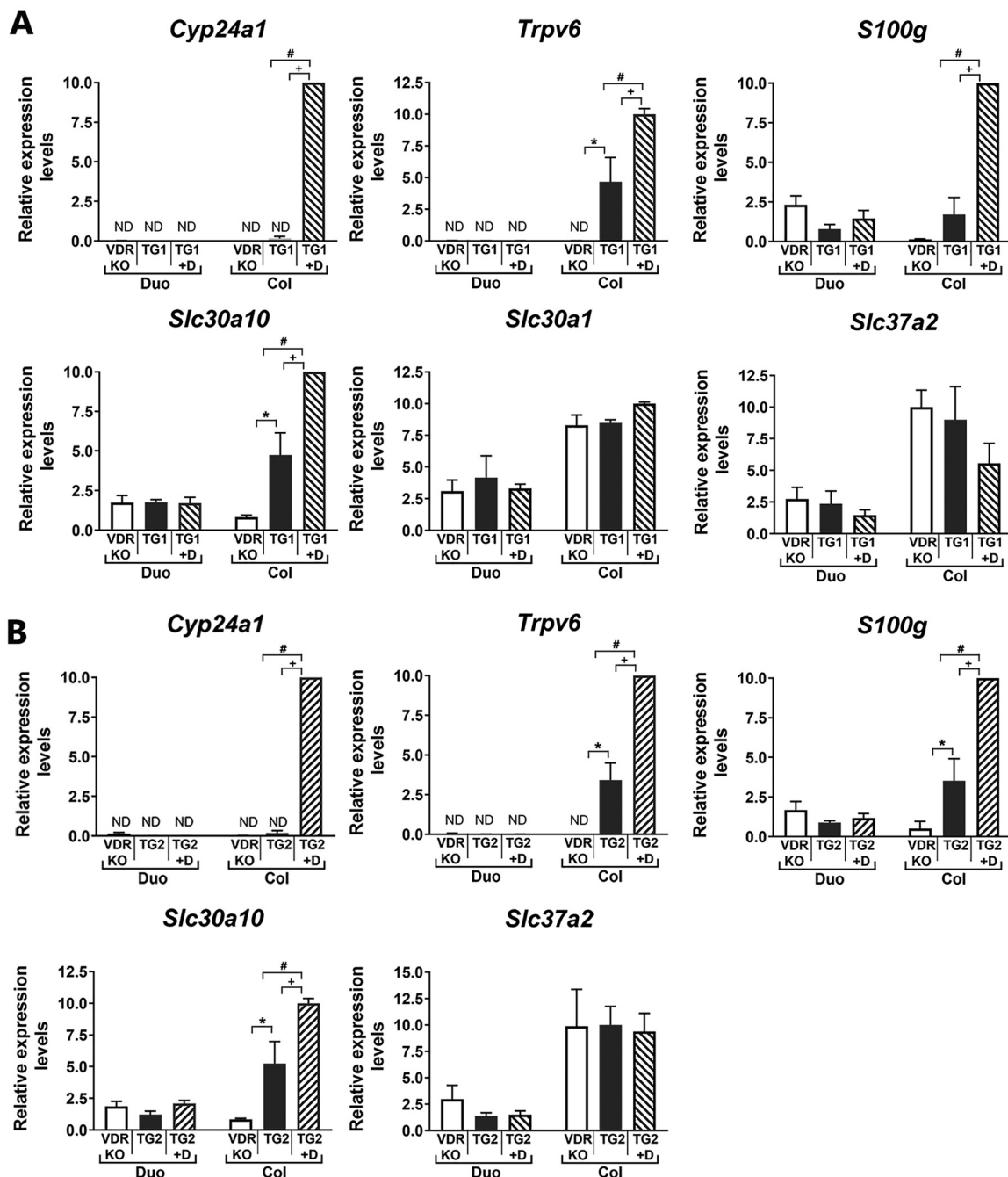


**FIG 2** Response to 1,25(OH)<sub>2</sub>D<sub>3</sub> treatment in KO/TG mouse intestine as measured by RT-qPCR. Gene expression in the duodenum (Duo) and colon (Col) of KO/TG1 mice (TG1) (A) or KO/TG2 mice (mice from a second transgenic line [TG2]) (B) treated with vehicle or 1,25(OH)<sub>2</sub>D<sub>3</sub> (1 ng/g body weight at 48, 24, and 6 h before termination; TG1 + D or TG2 + D). Results are compared to those from VDR KO mice. *n* = 6 per experimental group. Gene expression was normalized to *Gapdh* and expressed as means ± SEMs. +, *P* < 0.05 compared to vehicle (TG1 or TG2); #, *P* < 0.05 between 1,25(OH)<sub>2</sub>D<sub>3</sub> treated (TG1 or TG2 + D) and VDR KO; \*, *P* < 0.05 between vehicle (TG1 or TG2) and VDR KO. The duodenum was included as a control. Note the lack of responsiveness of the duodenum to 1,25(OH)<sub>2</sub>D<sub>3</sub> treatment due to the absence of VDR in the proximal intestine of these transgenic mice. ND, not detected.

manganese levels in blood, brain, and liver 20- to 60-fold higher than do controls (27). Expression of *S100g* and *Trpv6* was markedly decreased in the duodenum of the *Slc30a10*<sup>-/-</sup> mice (>10-fold) (Fig. 5A) but not significantly changed in the colon. Also, no change was observed in the duodenum and colon in the expression of *Tjp1* [ZO-1 gene; previous reports suggested regulation by 1,25(OH)<sub>2</sub>D<sub>3</sub> of intestinal tight junction protein ZO-1] (28). To determine the specificity for vitamin D-regulated calcium trans-

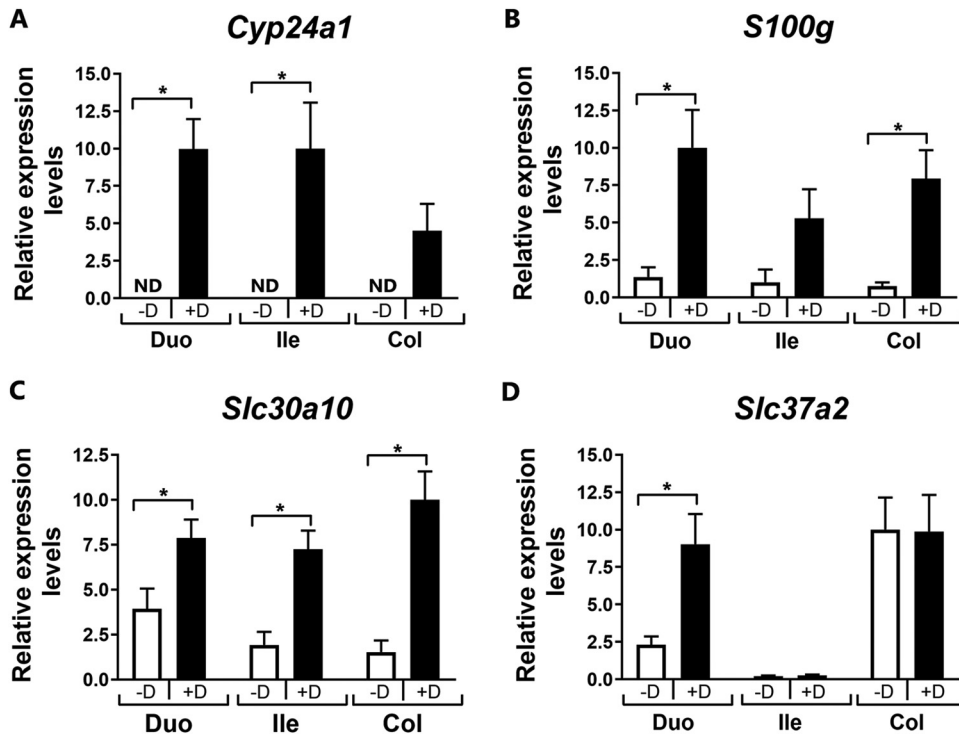


**FIG 3** Gene expression in intestinal segments in response to repeated administration of  $1,25(\text{OH})_2\text{D}_3$  to vitamin D-deficient mice. Twelve- to 14-week-old vitamin D-deficient mice were injected with  $1,25(\text{OH})_2\text{D}_3$  (+D) or vehicle (-D) three times over 48 h (at 48, 24, and 6 h prior to termination; i.p., 1 ng/g body weight per injection). Data were normalized to *Gapdh* and expressed as means  $\pm$  SEMs.  $n = 6$  per experimental group. \*,  $P < 0.05$  versus vehicle-treated group; Duo, duodenum; Ile, ileum; Col, colon; ND, not detected.

porters in the intestine, *Trpv5* and *S100g* were examined in the kidneys of *Slc30a10*<sup>-/-</sup> mice. Expression of *S100g* and *Trpv5* was unaffected in the kidney (Fig. 5B).

Micro-computed tomography ( $\mu\text{CT}$ ) analysis of the tibiae was performed to assess trabecular and cortical parameters in control and *Slc30a10*<sup>-/-</sup> mice. Trabecular bone mass was slightly, although not significantly, reduced in male *Slc30a10*<sup>-/-</sup> mice versus that in control mice, whereas no differences in trabecular bone mass were observed in female mice (Table 1). However, a strong cortical bone phenotype was observed in both male and female mice. Tibias of *Slc30a10*<sup>-/-</sup> mice were smaller in diameter than tibias of control mice as evidenced by their reduced cross-sectional tissue area. In addition, cortical thickness as well as cortical porosity were significantly reduced in *Slc30a10*<sup>-/-</sup> mice at middiaphysis (Table 1). Serum calcium levels were unchanged between *Slc30a10*<sup>-/-</sup> and control mice ( $12.5 \pm 1.3$  versus  $12.3 \pm 0.4$  ng/ml, respectively;  $P > 0.5$ ;  $n = 5$ ). Thus, in addition to the reduction in *Trpv6* and *S100g*, there was a significant bone phenotype in these mice.

**VDR and vitamin D target genes in mouse crypts and villi and in differentiated and undifferentiated human enteroids.** To provide insight into the mechanisms involved in the regulation of vitamin D target genes in the intestine, including the ion transporters, we examined both mouse villi and crypts. Additionally, human enteroid cultures were used to examine both undifferentiated (crypt-like) and differentiated (villus-like) responses to  $1,25(\text{OH})_2\text{D}_3$  and to determine whether the effects of  $1,25(\text{OH})_2\text{D}_3$  in the intestine observed in mice are conserved in humans. Although the importance of vitamin D-regulated proteins in intestinal villi has been reported, little is known about effects of  $1,25(\text{OH})_2\text{D}_3$  in crypts, and few findings related to human intestinal VDR targets have been reported. Crypts and villi were isolated from mouse duodenum using the EDTA chelation method (Fig. 6A). Expression of *Vdr* as well as VDR protein in mouse villus and crypt was equivalent (Fig. 6B). Both villus and crypt respond

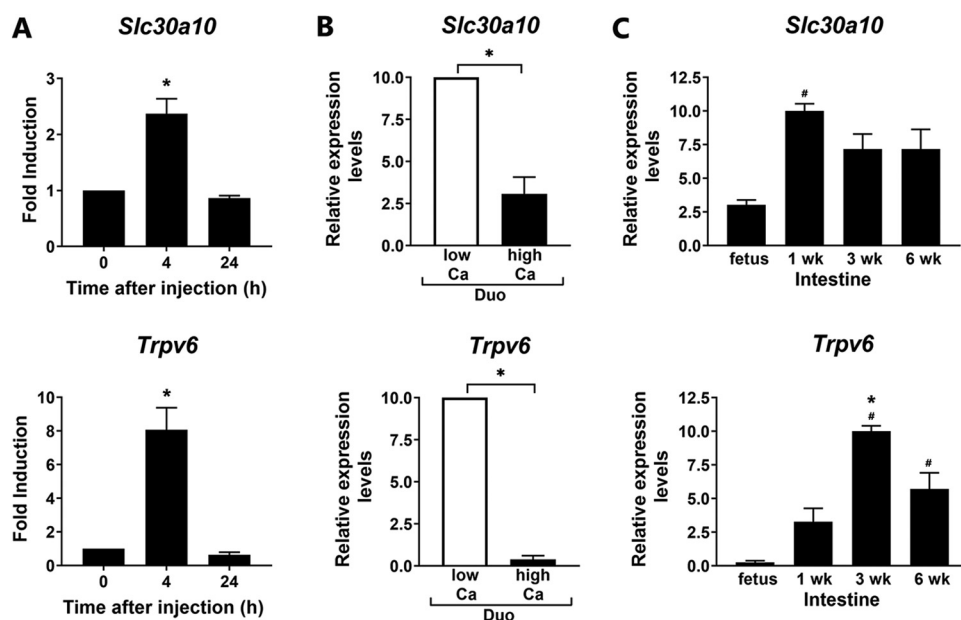
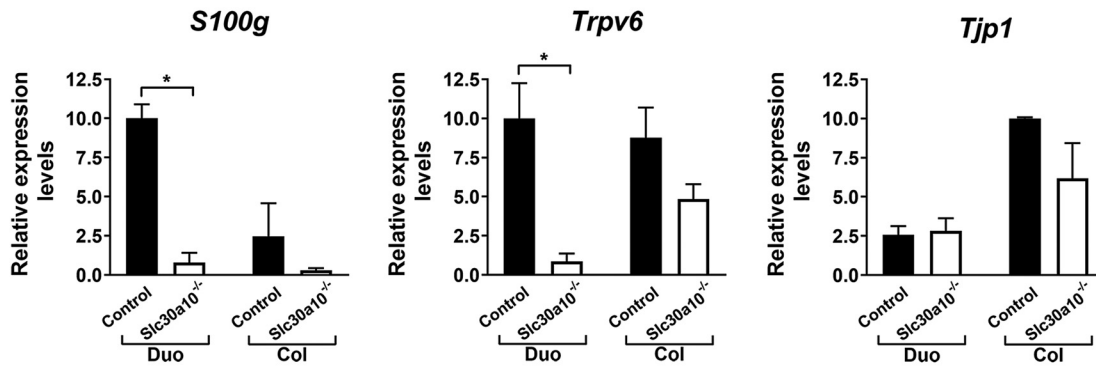


**FIG 4** Regulation of intestinal 1,25(OH)<sub>2</sub>D<sub>3</sub> target gene expression: time course of induction by 1,25(OH)<sub>2</sub>D<sub>3</sub>, effects of dietary calcium and developmental changes. (A) RT-qPCR analysis of *Slc30a10* and *Trpv6* expression in the duodenum at 0, 4, and 24 h after a single injection of 1,25(OH)<sub>2</sub>D<sub>3</sub> (10 ng/g body weight) to vitamin D-deficient mice.  $n = 5$  per time point. \*,  $P < 0.05$  compared to zero time point. (B) RT-qPCR analysis of *Slc30a10* and *Trpv6* expression in duodenum of mice fed a low-calcium (0.02%) or high-calcium (1%) diet for 4 weeks.  $n = 7$  per group. \*,  $P < 0.05$ . (C) Developmental changes in gene expression in mice raised under standard conditions and killed at 18 days gestation and at 1, 3, and 6 weeks of age. Intestine was harvested (for fetus,  $n = 5$ , pooled intestinal samples of 3 or 4 individual intestines;  $n = 5$  or 6 for 1-, 3-, and 6-week-old mice). Since the small intestine and not individual segments were harvested and analyzed in the fetus, for comparison, small intestine was also analyzed at different postnatal stages. Data are expressed as means  $\pm$  SEMs. Data were normalized using *Gapdh* or 18S rRNA. #,  $P < 0.05$  versus fetus; \*,  $P < 0.05$  versus 1-week-old rat; Duo, duodenum.

to 1,25(OH)<sub>2</sub>D<sub>3</sub> by inducing expression of *Cyp24a1* (Fig. 6C). *Slc30a10* and *Trpv6*, although more pronounced in villi, were also expressed in crypts of WT mice (Fig. 6D).

RNA-seq analysis of human duodenal enteroids (Fig. 7) showed that intestinal vitamin D target genes are conserved in humans. Similar to the findings in mice, expression of *VDR* under basal conditions was equivalent in villus and crypt compartments. The expression of *VDR* was not significantly affected by 1,25(OH)<sub>2</sub>D<sub>3</sub>. However, *TRPV6*, *SLC30A10*, *CYP24A1*, and *ATP2B1* were significantly upregulated upon 1,25(OH)<sub>2</sub>D<sub>3</sub> treatment in both villus and crypt (Fig. 7C). *S100G* was significantly induced by 1,25(OH)<sub>2</sub>D<sub>3</sub> only in villus-like cultures. A similar regulation of vitamin D target genes was observed in crypt-like and villus-like human enteroids derived from the colon (data not shown). Expression of *SLC* transporter genes in addition to *SLC30A10* in differentiated and undifferentiated human duodenal enteroids treated with 1,25(OH)<sub>2</sub>D<sub>3</sub> or vehicle is shown in Table 2. *SLC30A4* and *SLC30A5* were not significantly affected by 1,25(OH)<sub>2</sub>D<sub>3</sub>. *SLC37A2* was induced in villus but not in crypts. The intestinal phosphate transporter, encoded by *SLC34A2*, was upregulated by 1,25(OH)<sub>2</sub>D<sub>3</sub> in both villus and crypt. Expression of *TRPM7*, a non-*SLC* gene transporter, was unaffected by 1,25(OH)<sub>2</sub>D<sub>3</sub> treatment. Gene ontology (GO) analysis was performed to identify biological processes, cellular components, and molecular function terms that are enriched in human duodenal enteroids treated with 1,25(OH)<sub>2</sub>D<sub>3</sub>. The enrichment scores ( $-\log_{10}$  [P value]) of the terms were plotted to indicate the significance of the enrichment of each function. Regulation of epithelial cell differentiation represented a major category for enrichment of genes by 1,25(OH)<sub>2</sub>D<sub>3</sub> in crypts (Fig. 8). *Sonic hedgehog* (*SHH*), which controls the proliferation of stem cells, was a 1,25(OH)<sub>2</sub>D<sub>3</sub> target gene in this ontology group and is expressed in response to nutrients, cell migration, and cell motility, indicating a role for 1,25(OH)<sub>2</sub>D<sub>3</sub> in the function of stem cells. Pathway analysis indicated enrichment of genes by 1,25(OH)<sub>2</sub>D<sub>3</sub> involved in ion transport,

**A Intestine**



**B Kidney**

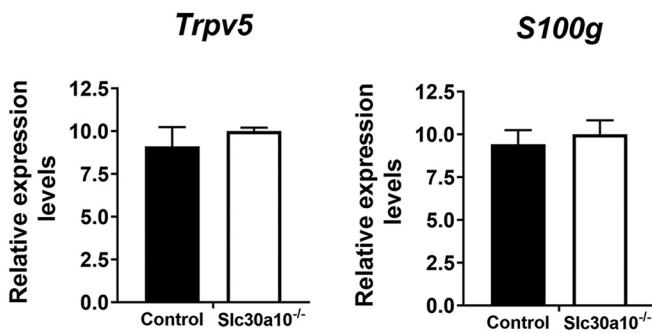


**FIG 5** 1,25(OH)<sub>2</sub>D<sub>3</sub> target gene expression in the intestine (A) and kidney (B) of *Slc30a10*<sup>-/-</sup> and control mice. Data are expressed as means ± SEMs and were normalized using *Gapdh*. *n* = 4 to 6 in each group. \*, *P* < 0.05; Duo, duodenum; Col, colon.

oxidation reduction, vitamin D 24-hydroxylase activity, and steroid metabolic processes as well as in calcium ion binding, and microsomes and vesicular fraction were categories shared in both villus and crypt (Fig. 8). 1,25(OH)<sub>2</sub>D<sub>3</sub> target gene members of the gene ontology group identifying microsomes and vesicular fraction included *CYP3A4*, which is involved in vitamin D metabolism, and *CYP2C19* and *CYP2C18*, which are involved in drug metabolism.

**TABLE 1** Trabecular and cortical bone parameters of control and *Slc30a10* KO mice

Parameter <sup>a</sup>	Value in <sup>b</sup> :			
	Male mice		Female mice	
	Control	Slc30a10 KO	Control	Slc30a10 KO
<b>Trabecular bone</b>				
<i>n</i>	8	5	10	9
BV/TV <sup>c</sup> (%)	6.55 ± 1.60	4.44 ± 1.29	5.41 ± 2.33	4.72 ± 1.20
Trabecular no. (per mm)	2.07 ± 0.39	1.48 ± 0.36 <sup>d</sup>	1.62 ± 0.57	1.54 ± 0.35
Trabecular thickness (mm)	0.031 ± 0.002	0.030 ± 0.002	0.033 ± 0.002	0.031 ± 0.001 <sup>d</sup>
<b>Cortical bone</b>				
<i>n</i>	8	4	10	8
Cross-sectional tissue area (mm <sup>2</sup> )	2.11 ± 0.30	1.35 ± 0.39 <sup>d</sup>	1.92 ± 0.27	1.33 ± 0.16 <sup>d</sup>
Medullary area (mm <sup>2</sup> )	1.44 ± 0.23	1.00 ± 0.34 <sup>d</sup>	1.29 ± 0.23	1.03 ± 0.13 <sup>d</sup>
Cortical thickness (mm)	0.124 ± 0.012	0.092 ± 0.023 <sup>d</sup>	0.140 ± 0.011	0.086 ± 0.010 <sup>d</sup>
Porosity (%)	12.07 ± 2.68	6.12 ± 1.12 <sup>d</sup>	9.22 ± 2.07	6.24 ± 1.55 <sup>d</sup>

<sup>a</sup>Trabecular bone parameters and cortical bone parameters as measured by μCT.

<sup>b</sup>Data are presented as means ± SEMs (unpaired, two-tailed *t* test KO versus WT for each sex).

<sup>c</sup>BV/TV, bone volume/tissue volume.

<sup>d</sup>*P* < 0.05.



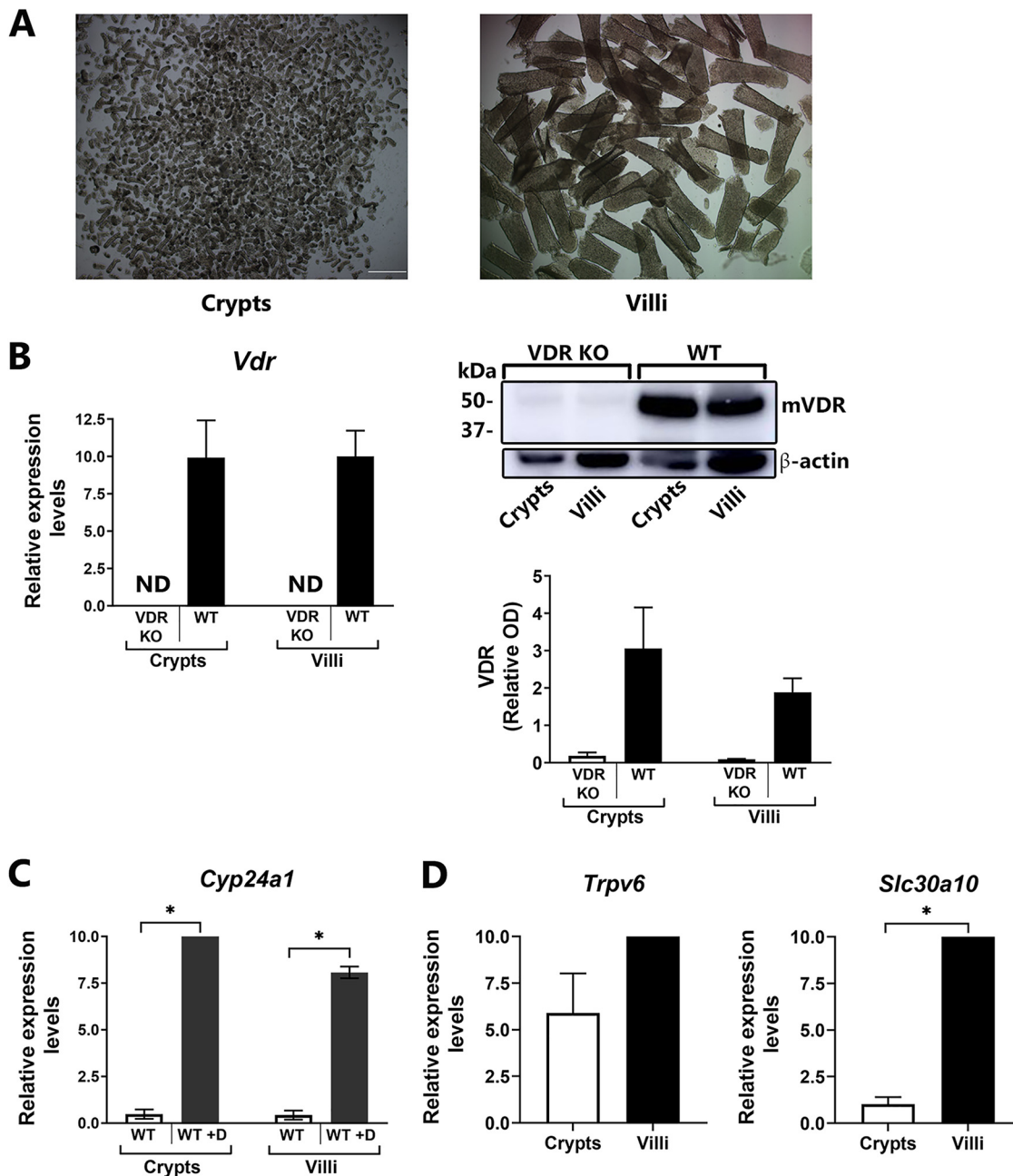


**FIG 6** VDR and 1,25(OH)<sub>2</sub>D<sub>3</sub> target genes in mouse epithelial cells in villi and crypts. (A) Intestinal epithelial cells were isolated from crypts (left) and villi (right) of 3-month-old mouse duodenum. (B) *Vdr* gene expression (left) and VDR protein (Western blot analysis; right) in mouse duodenal crypts and villi from 3-month-old WT mice compared to that in VDRKO mice. For Western blot analysis, the relative optical density (OD) obtained using the VDR antibody was divided by the OD obtained after  $\beta$ -actin staining to produce VDR-relative OD.  $n = 3$  or 4. (C and D) RT-qPCR analysis of 1,25(OH)<sub>2</sub>D<sub>3</sub> target genes in mouse duodenal villi and crypts. (C) *Cyp24a1* expression was examined in 3-month-old mice injected i.p. with vehicle or 1,25(OH)<sub>2</sub>D<sub>3</sub> (1 ng/g body weight; injected at 48, 24, and 6 h prior to euthanasia). \*,  $P < 0.05$ . (D) *Trpv6* and *Slc30a10* gene expression in intestinal epithelial cells from crypts and villi of 3-month-old WT mice. RT-qPCR results were normalized to *Gapdh* or 18S rRNA.  $n = 3$  or 4. ND, not detected.

**DISCUSSION**

Vitamin D plays a major role in maintaining the integrity and function of the intestine as well as in the control of calcium homeostasis. However, the mechanisms by which 1,25(OH)<sub>2</sub>D<sub>3</sub> regulates these processes are not fully understood. Our findings indicate the importance of the distal as well as the proximal segments of the intestine to understand the intestinal effects of 1,25(OH)<sub>2</sub>D<sub>3</sub> and show that 1,25(OH)<sub>2</sub>D<sub>3</sub>-

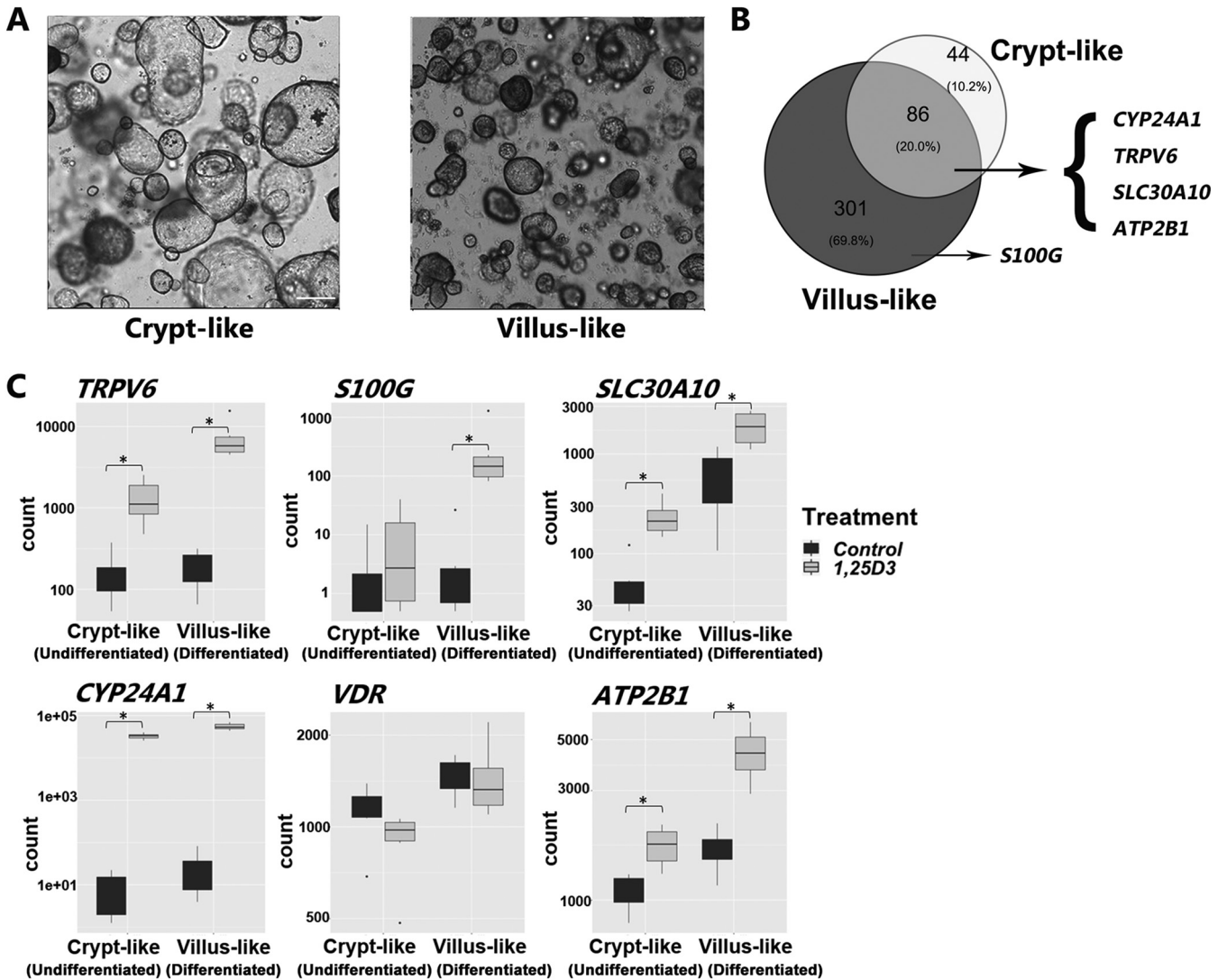


**FIG 7** Gene expression measured by RNA-seq in crypt-like and villus-like human duodenal enteroids. (A) Bright-field images of crypt-like (undifferentiated) and villus-like (differentiated) duodenal human enteroids. (B) Venn diagram indicating genes significantly upregulated at least 1.5-fold and with a false-discovery rate [FDR] of <0.05 upon 1,25(OH)<sub>2</sub>D<sub>3</sub> treatment (100 nM for 24 h) in crypt-like (undifferentiated) and villus-like (differentiated) human enteroids and overlapping genes. (C) Expression counts of *SLC30A10*, *VDR*, and classic 1,25(OH)<sub>2</sub>D<sub>3</sub> target genes in control and 1,25(OH)<sub>2</sub>D<sub>3</sub>-treated villus and crypt-like human enteroids. Data are from enteroids from 6 patients (3 female and 3 male).

mediated responses involve epithelial cells in the crypts as well as the villus. This study also shows that the effects of 1,25(OH)<sub>2</sub>D<sub>3</sub> on intestine are complex, are conserved in humans for active calcium uptake, and include calcium-regulating as well as calcium-independent effects in both proximal and distal intestine.

**TABLE 2** Gene expression of transporters in crypt-like and villus-like human enteroids derived from duodenum treated with 1,25(OH)<sub>2</sub>D<sub>3</sub> or vehicle

Gene	Crypt-like enteroid		Villus-like enteroid		Description
	Fold change	P value	Fold change	P value	
<i>SLC30A10</i>	5.38	2.05E-19 <sup>a</sup>	3.20	2.99E-03 <sup>a</sup>	Mn efflux transporter
<i>SLC30A4</i>	0.82	5.51E-01	0.93	8.44E-01	Zn transporter
<i>SLC30A5</i>	1.02	9.56E-01	1.05	7.89E-01	Zn transporter
<i>SLC34A2</i>	6.94	5.17E-22 <sup>a</sup>	3.02	3.00E-03 <sup>a</sup>	Phosphate transporter
<i>SLC37A2</i>	1.06	9.63E-01	13.13	8.34E-49 <sup>a</sup>	G6P transporter
<i>TRPM7</i>	0.94	9.22E-01	0.78	1.23E-01	Non-SLC transporter of divalent cations

<sup>a</sup>P < 0.05.

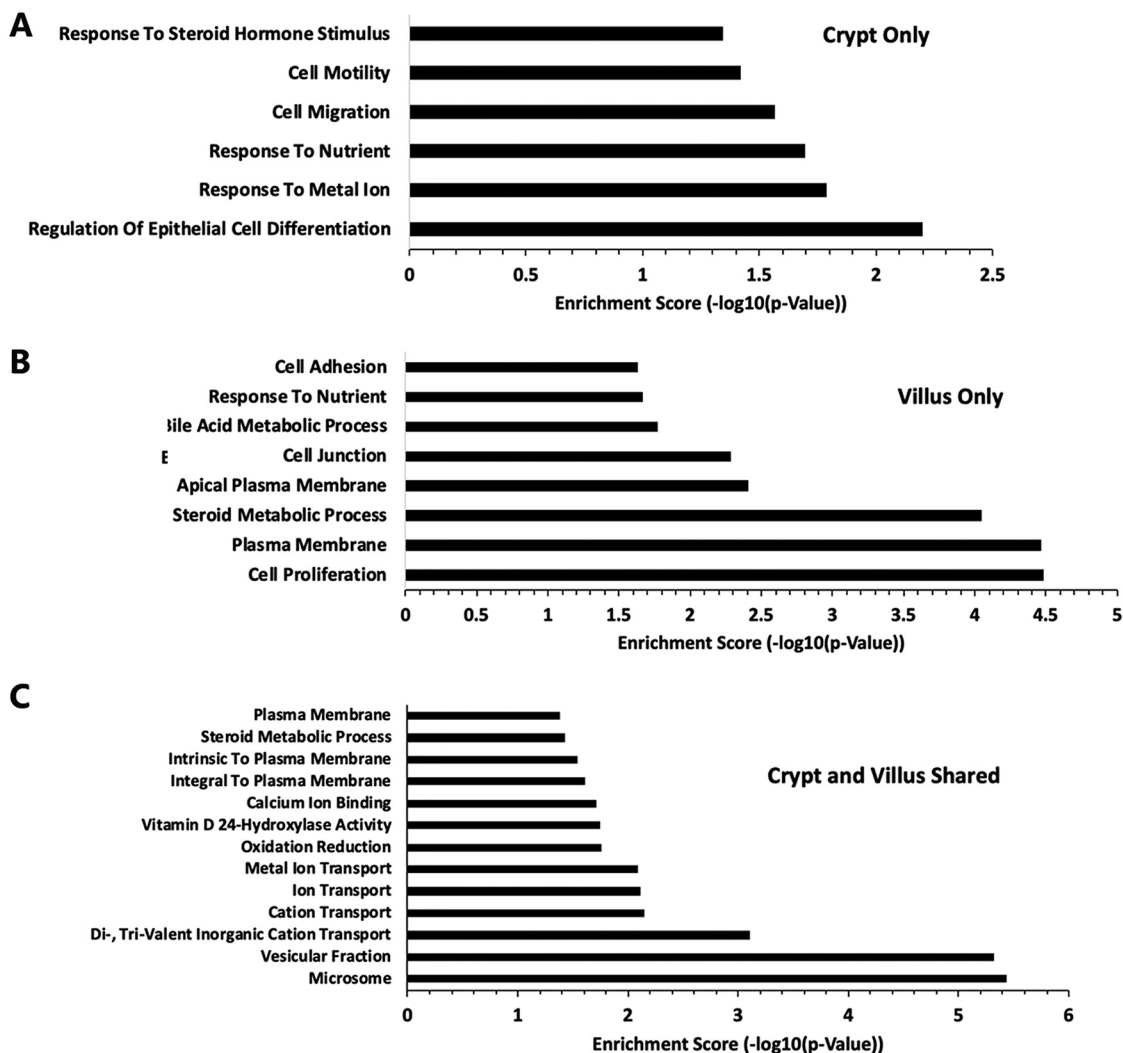


**FIG 8** Top GO terms for genes enriched in human duodenal enteroids treated with 1,25(OH)<sub>2</sub>D<sub>3</sub>. (A) Crypt only; (B) villus only; (C) crypt and villus shared.

Previous investigations reported that 1,25(OH)<sub>2</sub>D<sub>3</sub>-mediated active calcium transport was localized only in the duodenum, where the most pronounced effects of 1,25(OH)<sub>2</sub>D<sub>3</sub> during the active calcium transport process were induction of calbindin-D<sub>9k</sub> (*S100g*) and *Trpv6* (4, 5, 9). Our current findings indicate that the classic 1,25(OH)<sub>2</sub>D<sub>3</sub>-activated genes (*S100g* and *Trpv6*) are also the two genes most markedly induced by 1,25(OH)<sub>2</sub>D<sub>3</sub> in the distal intestine (similar to previous findings in the proximal intestine). In addition, our recent study showing, for the first time, a similar VDR-dependent calcium absorption efficiency between proximal colon and duodenum in the same mouse further establishes a role for the distal intestine in VDR-mediated intestinal calcium absorption (29). In that study, calcitriol glycosides and glucuronides, which target calcium absorption in the distal intestine, were also found to upregulate *Trpv6* and *S100g* (the genes involved in active calcium transport) as well as calcium absorption in the colon. These results which provide direct *in vivo* evidence for the importance of VDR in the distal intestine suggest, together with earlier studies (11–14), that active calcium transport is a vitamin D-dependent process in the distal intestine, which plays a role in calcium homeostasis. Calcitriol glucuronide treatment may be a means to target calcitriol to the distal intestine and thus compensate for the loss of calcium absorption, for example, by gastric bypass surgery or small bowel resection. In the present investigation, specific genes previously associated with paracellular calcium

transport were not significantly changed by  $1,25(\text{OH})_2\text{D}_3$  in mouse distal intestine. However, *Cldn2* was significantly induced by  $1,25(\text{OH})_2\text{D}_3$  in the duodenum. Although it is possible that  $1,25(\text{OH})_2\text{D}_3$  is involved in paracellular as well as active calcium transport, the physiological relevance of the reported regulation of genes by  $1,25(\text{OH})_2\text{D}_3$  involved in paracellular transport remains to be determined (6, 7, 18).

Compared to that in other tissues, the highest levels of VDR are found in the small and large intestine. Studies related to  $1,25(\text{OH})_2\text{D}_3$ -mediated responses have focused on effects in differentiated enterocytes and have supported a role for  $1,25(\text{OH})_2\text{D}_3$  in intestinal calcium absorption as well as barrier function (4–7). However, the effect of  $1,25(\text{OH})_2\text{D}_3$  on intestinal stem cells has not been well investigated and has been a matter of debate (20–22). Previous studies using oral treatment reported that  $1,25(\text{OH})_2\text{D}_3$  stimulates *Cyp24a1* in intestinal epithelial cells at the villus or tip region and not at the crypts (20). Early microscopic autoradiographic studies, however, noted that tritium-labeled  $1,25(\text{OH})_2\text{D}_3$  concentrated in both absorptive and crypt epithelial cells in the small and large intestines (30, 31). Using a highly specific and sensitive VDR antibody (D6) (32), we also noted, similar to in the autoradiographic studies, that VDR is present in villus and crypts. Our studies using isolated mouse villus and crypt as well as human enteroids with either a crypt-like phenotype (high proliferation, undifferentiated) or a villus-like phenotype (low proliferation, differentiated) identified  $1,25(\text{OH})_2\text{D}_3$ -induced target genes, including *Cyp24a1*, in both villus and crypts. The importance of vitamin D in the function of *Lgr5*<sup>+</sup> stem cells, which are sensitive to Wnt stimulation and contribute to intestinal homeostatic regeneration, was previously noted by L. Augenlicht's lab (22). They showed that inactivation of the VDR in mouse *Lgr5*<sup>+</sup> intestinal crypt base columnar cells compromised stem cell functions of the *Lgr5*<sup>+</sup> cells (22). Studies in human colon crypt organoids have also provided evidence that VDR is expressed in intestinal stem cells and has a regulatory role, as  $1,25(\text{OH})_2\text{D}_3$  was found to induce stemness-related genes and to inhibit genes involved in cell proliferation (33). We are now only beginning to understand the regulatory role of vitamin D in intestinal stem cells (22, 33, 34). It is of interest that, in our *in vivo* studies in mice as well as in our studies using human enteroids,  $1,25(\text{OH})_2\text{D}_3$  was found to regulate classic target genes in both villus and crypt. These findings suggest, similar to early studies showing the time dependency of  $1,25(\text{OH})_2\text{D}_3$  action in enterocytes during their differentiation (35), that  $1,25(\text{OH})_2\text{D}_3$  action in the intestine involves not only calcium absorption but also cellular differentiation and intestinal homeostasis. Although there have been many studies related to the intestinal effects of vitamin D in animals, ours is one of the few studies examining human vitamin D target genes. Previous studies have been conducted using human intestinal cell lines derived from colon (19, 36–38) as well as human biopsy specimens and duodenal explants (39, 40). The limitation of the studies in explants is the inability of the cells to renew as well as cell death in the explants. The enteroid culture system from human tissue allows growth and maintenance over time and provides an important *in vitro* model to examine both stem and non-stem cell responses to  $1,25(\text{OH})_2\text{D}_3$ . These epithelial cultures of the intestinal tract will provide technology enabling the verification of findings observed in animals and the identification of key components involved in  $1,25(\text{OH})_2\text{D}_3$  action in human intestinal biology.

In addition to *Cyp24a1*, *Trpv6*, and *S100g*, *Slc30a10*, encoding a manganese efflux transporter, is also a  $1,25(\text{OH})_2\text{D}_3$  target gene in both proximal and distal intestine. *Slc30a10* is localized in the apical/luminal domain of the intestine, in liver, and in brain (41). Although initially thought to act as a Zn efflux transporter, recent studies have identified *SLC30A10* as a mediator of Mn efflux which lowers cellular Mn levels and protects against Mn toxicity (23, 27, 42, 43). In clinical studies, patients carrying homozygous mutations in *SLC30A10* show enhanced Mn levels, neurotoxicity, and liver injury (43, 44). It is of interest that Mn levels in the brain are minimally elevated in liver-specific *Slc30a10* KO mice (41, 45). However, endoderm-specific KO mice (lacking *Slc30a10* in liver and the gastrointestinal tract) were found to have markedly elevated Mn levels in the brain, indicating a critical role for the digestive system in the regulation

of brain manganese (41, 45). Our results suggest that 1,25(OH)<sub>2</sub>D<sub>3</sub>, by inducing *Slc30a10* in the intestine, may increase Mn excretion and thus may have therapeutic benefit without direct effects on the brain. Preliminary data comparing mice injected with MnCl<sub>2</sub> (15 μg/g body weight) alone or MnCl<sub>2</sub> plus 1,25(OH)<sub>2</sub>D<sub>3</sub> (1 ng/g body weight) 3 times per week for 3 weeks showed that 1,25(OH)<sub>2</sub>D<sub>3</sub> treatment results in decreased levels of blood Mn (control, 30 ± 2.3ng Mn/ml; MnCl<sub>2</sub> treated, 403 ± 91ng Mn/ml; MnCl<sub>2</sub> plus 1,25(OH)<sub>2</sub>D<sub>3</sub> treated, 288 ± 3.3 ng Mn/ml) (S. Mukhopadhyay and S. Christakos, preliminary results). Further studies will be needed to determine effects of 1,25(OH)<sub>2</sub>D<sub>3</sub> on neurotoxicity and on levels of Mn in different tissues as well as the effects of vitamin D deficiency, dietary calcium, and high-dose dietary vitamin D on Mn toxicity. Although elevated levels of Mn are neurotoxic, Mn is an essential element which plays a role in many cellular processes (46). With regard to bone homeostasis, it has been reported that the skeleton is positively influenced by Mn and that deficiency in Mn affects bone mass. Studies in rats have shown that Mn supplementation inhibits ovariectomy-induced bone loss (47). In addition, plasma levels of Mn were reported to be significantly decreased in groups of osteoporotic patients (48). More recent studies have noted that local manganese chloride treatment accelerates fracture healing in a rat model (49). However, excess of Mn can adversely affect bone quality. In our study using the *Slc30a10* global KO mouse, which exhibits marked elevations in blood Mn, significant cortical bone abnormalities were noted. These findings further indicate the importance of maintaining Mn levels at an optimal range and not exceeding the levels required to accomplish essential functions. The mechanisms involved in the adverse effects on bone observed in the *Slc30a10* KO mouse are not known. Whether the reduced thyroxine production observed in the *Slc30a10*KO mouse plays a role in the bone phenotype remains to be determined (50). The precise mechanism whereby Mn affects thyroxine biosynthesis is not known. It is of interest that a patient with a loss-of-function *SLC30A10* mutation was also identified with hypothyroidism (51).

Due to the necessity of maintaining Mn levels in a narrow range in order to prevent toxicity, understanding the regulation of *SLC30A10* is critical. The regulation of *Slc30a10* in the intestine by 1,25(OH)<sub>2</sub>D<sub>3</sub> suggests that 1,25(OH)<sub>2</sub>D<sub>3</sub> not only affects absorption of calcium but also may affect the transport of other divalent cations. The time course of response to 1,25(OH)<sub>2</sub>D<sub>3</sub> showed that expression of *Trpv6* and *Slc30a10* is significantly elevated 4 h after 1,25(OH)<sub>2</sub>D<sub>3</sub>. Twenty-four hours after administration of 1,25(OH)<sub>2</sub>D<sub>3</sub>, the expression of the genes for both transporters was decreased to levels observed prior to 0 h, consistent with a rapid response of both transporters to 1,25(OH)<sub>2</sub>D<sub>3</sub>, as previously noted for *Trpv6* expression (52). The early induction of these transporters would be needed for rapid calcium uptake or Mn efflux. Although putative vitamin D response elements have been noted in the human and mouse genes which encode *SLC30A10* (18, 19), studies are needed to determine VDR binding sites which are functionally linked to the expression of these genes. The significance of a possible inhibitory effect of unliganded VDR also requires further studies (53, 54).

To further understand the role of vitamin D in manganese homeostasis, the expression of the classic vitamin D target genes was examined in the intestine of the *Slc30a10* KO mouse. In the *Slc30a10* KO mouse, a marked decrease in the expression of *Trpv6* and *S100g* in the duodenum, a primary route of manganese excretion (55), was consistently observed. These findings suggest that TRPV6, S100G, and *SLC30A10* may work together in manganese efflux transport. Previous studies using HEK cells transfected with human (h) *TRPV6* showed that TRPV6 is permeable to Mn as well as other heavy metal cations, indicating that TRPV6 is involved not only in calcium transport (56). Since intracellular calcium concentrations have been reported to correlate with the level of expression of TRPV6 (56), our findings of a decrease in *Trpv6* (and *S100g*) in the intestine of mice with *Slc30a10* deficiency and defective Mn excretion suggest the possibility of intracellular calcium-mediated regulation of intestinal *Slc30a10*. Kovacs et al. observed an inhibition of calcium uptake mediated by TRPV6 in the presence of high concentrations of Mn (56). Therefore, it is also possible that low levels of expression of the genes involved in calcium homeostasis are due to the high Mn levels in the *Slc30a10* KO mice. Although

not previously identified *in vivo* in the intestine, an interrelationship between calcium and Mn transport has been noted in other reports, including studies in mast cells, in mitochondria, and in brain (57–62). It has been suggested that Mn may interfere with brain calcium homeostasis (62). In the mitochondria, Mn transport has been reported to be activated by calcium (58, 60). However, calcium transport in the mitochondria is inhibited in the presence of Mn (58). In recent studies using HEK cells, it was noted that Slc30a10 extrusion of Mn was calcium dependent (63). The authors suggested that Slc30a10 uses a calcium gradient for active counter-ion exchange (63). Whether Mn efflux transport is regulated in part by calcium in the intestine (as suggested by our findings) and intestinal calcium transport is inhibited in the presence of high blood Mn levels (which are observed in the Slc30a10 KO mouse) remain to be determined. It is possible that the role of the distal intestine, where *Slc30a10* is also induced by  $1,25(\text{OH})_2\text{D}_3$ , is compensatory when Mn efflux from the proximal intestine is disrupted. The relationship between calcium, the vitamin D endocrine system, and Mn efflux in the intestine is an unexplored topic. Since the digestive system has recently been identified as a critical regulator of Mn toxicity (41, 45), further studies are needed to provide new insight on the role of calcium and vitamin D on Mn homeostasis and protection against neurotoxicity.

Findings in our lab as well as prior reports have noted that  $1,25(\text{OH})_2\text{D}_3$  treatment affects the gene expression of intestinal transporters in addition to *Slc30a10*. Expression of *Slc37a2*, which encodes a phosphate-linked glucose 6 phosphate antiporter, was previously shown to be induced by  $1,25(\text{OH})_2\text{D}_3$  in mouse intestine (18). Although not regulated by  $1,25(\text{OH})_2\text{D}_3$  in the mouse distal intestine, we found that *SLC37A2* was induced by  $1,25(\text{OH})_2\text{D}_3$  in human enteroids from duodenum (Table 2) and colon (data not shown). Regulation of *SLC37A2* by  $1,25(\text{OH})_2\text{D}_3$  is not specific to the intestine. *SLC37A2* has also been suggested as a gene target and marker of vitamin D status in hematopoietic cells (64). Although *SLC37A2* can transport glucose 6 phosphate (G6P), recent findings suggested that *SLC37A2* does not have a role in the regulation of blood glucose (65). Since the functional role of *SLC37A2* is not understood at this time, the physiological significance of regulation of gene expression by  $1,25(\text{OH})_2\text{D}_3$  in both mouse and human intestines remains to be determined. Although we did not find that  $1,25(\text{OH})_2\text{D}_3$  affected major Zn transporters, previous studies noted regulation of zinc transporters by  $1,25(\text{OH})_2\text{D}_3$  in mouse intestine (18). Both calcium and zinc are known to play important roles in normal development and bone homeostasis (66–68). Early studies in chicks, however, noted that vitamin D or  $1,25(\text{OH})_2\text{D}_3$  does not affect zinc absorption in zinc-deficient or -replete animals (69). Due to the importance of zinc as well as calcium for skeletal integrity, further studies are needed to determine an interrelationship between vitamin D and zinc and whether vitamin D has an effect on zinc homeostasis. In addition to regulation of *SLC30A10* as well as *SLC37A2*, *SLC34A2*, encoding the intestinal cotransporter  $\text{NaP}_i\text{-IIb}$ , was noted to be a gene target induced by  $1,25(\text{OH})_2\text{D}_3$  in human enteroids derived from duodenum (*SLC34A2* is expressed in the proximal intestine in humans and primarily in the ileum in mice).  $1,25(\text{OH})_2\text{D}_3$  is known to stimulate intestinal phosphate absorption (70), and *SLC34A2* has been reported to protect bone when dietary phosphate is restricted (71). However, the role of  $1,25(\text{OH})_2\text{D}_3$  in the regulation of intestinal *SLC34A2* ( $\text{NaP}_i\text{-IIb}$ ) has been a matter of debate (72–74). Further studies are needed to examine the regulation of this phosphate transporter in human intestine, its physiological significance in bone and phosphate homeostasis in humans, and whether it has a role in the dysregulation of phosphate observed in chronic kidney disease.

In a recent study, intestine-specific knockout of *Trpm7*, which encodes a channel kinase suggested to control magnesium levels, resulted in decreased serum zinc and calcium levels as well as decreased serum magnesium by postnatal day 5 (mice died by postnatal day 10) (25). The authors suggested that *TRPM7* is the common gatekeeper for these ions in the intestine and that *TRPM7* and not *TRPV6* is the key factor in intestinal calcium absorption. However, these findings were observed in mice prior to the onset of vitamin D receptor-mediated active intestinal calcium absorption (which

occurs at weaning). In addition, results of our transcriptomic analyses did not indicate regulation of *Trpm7* by 1,25(OH)<sub>2</sub>D<sub>3</sub> in the intestine of mice, and *TRPM7* expression was unaffected by 1,25(OH)<sub>2</sub>D<sub>3</sub> treatment in human enteroids. Thus, although TRPM7 is important in early postnatal life, TRPV6 and not TRPM7 is involved in the process of 1,25(OH)<sub>2</sub>D<sub>3</sub>-regulated intestinal calcium absorption.

In summary, our findings suggest the importance of the distal as well as the proximal intestinal segments in order to understand intestinal effects of vitamin D and show that 1,25(OH)<sub>2</sub>D<sub>3</sub> effects involve intestinal epithelial cells in both the villus and crypt. In addition, our findings show direct transcriptomic responses to 1,25(OH)<sub>2</sub>D<sub>3</sub> in human enteroids in both villus and crypt and that effects observed in mice are conserved in humans. Since SLC30A10 is the first reported transporter that uses a calcium gradient for active counter-ion exchange, our findings suggest that TRPV6, S100G, and SLC30A10 work together in Mn transport and that 1,25(OH)<sub>2</sub>D<sub>3</sub> may have a role not only to maintain calcium homeostasis but also in the cellular homeostasis of other divalent ions.

## MATERIALS AND METHODS

**Animals.** Studies including the use of wild-type (C57BL/6J), KO/TG (mice expressing VDR only in the distal intestine), and *Vdr* knockout (KO) mice were approved by the Rutgers, New Jersey Medical School Animal Care and Use Committee. Mice were maintained in a virus and parasite-free barrier facility and exposed to a 12-h light/12-h dark cycle. Food and water were given *ad libitum*.

Transgenic mice expressing VDR only in the distal intestine were generated as previously described (14) using a 9.5-kb fragment from the CDX2 promoter, which directs transgene expression specifically to the distal intestine (75). The pBSKS-9.5 kb CDX2-human(h)VDR poly(A) transgene was injected into pronuclei of fertilized mouse oocytes at the Rutgers New Jersey Medical School Genome Editing Core Facility. Mice heterozygous for transgene integration and ablation of the endogenous VDR (TG<sup>+/-</sup>/KO<sup>+/-</sup>) were bred to obtain mice with distal intestine-specific hVDR expression (TG/KO mice) (Fig. 1A). All TG/KO mice were fed standard rodent chow diet (Rodent Laboratory Chow 5001; Ralston Purina Co.) and were used at 12 to 14 weeks of age. Genotyping was performed by PCR using DNA extracted from tail biopsy specimens and mouse- and human-specific VDR primers (14). VDR KO mice were obtained from the Jackson Laboratory (originally from M. Demay, Harvard Medical School).

Findings in the TG/KO mouse intestine were compared to results obtained using vitamin D-deficient mice. To examine the response to 1,25(OH)<sub>2</sub>D<sub>3</sub> in both TG/KO mice and vitamin D-deficient mice, each animal was administered three intraperitoneal injections of vehicle or 1,25(OH)<sub>2</sub>D<sub>3</sub> (Cayman Chemical Company, Ann Arbor, MI) at a concentration of 1 ng/g body weight in a 9:1 mix of propylene glycol and ethanol at 48, 24, and 6 h before termination. The three-dose protocol was used to study short-term and long-term effects of 1,25(OH)<sub>2</sub>D<sub>3</sub> administration.

The vitamin D-deficient mice were generated from C57BL/6J female mice fed a vitamin D deficient diet (-D) (0.47% Ca, 0.3% P; TD89123; Teklad diet from Envigo) for 3 to 4 weeks before mating and during pregnancy and lactation. Their offspring were provided the same diet starting directly after weaning until the tissues were harvested at 12 to 14 weeks of age.

Slc30a10 KO (*Slc30a10*<sup>-/-</sup>) mice were generated in the lab of Somshuvra Mukhopadhyay as previously described (27). Tissues from *Slc30a10*<sup>-/-</sup> mice were obtained at the University of Texas at Austin (UT Austin) under protocols approved by the Institutional Animal Care and Use Committee at UT Austin. Animals were fed regular rodent chow containing ~84 μg Mn/g, and tissues were harvested at 5 to 6 weeks of age, as knockouts develop severe Mn toxicity beyond 8 weeks of age.

To compare the regulation of Slc30a10 to the regulation of classic 1,25(OH)<sub>2</sub>D<sub>3</sub> target genes, a time course of response to 1,25(OH)<sub>2</sub>D<sub>3</sub> as well as the response to high- or low-calcium diets and developmental changes in the expression of *Slc30a10* were examined. The time course study was conducted using vitamin D-deficient mice injected with a single dose of 1,25(OH)<sub>2</sub>D<sub>3</sub> (intraperitoneal [i.p.], 10 ng/g body weight) and killed at 1, 4, or 24 h after injection. The dietary study was conducted using 4-week-old mice fed either a high-calcium (1% Ca; TD92309) or low-calcium (0.02% Ca; TD86162) diet for 4 weeks. For the developmental study, timed pregnant, neonatal, and adult mice were fed a standard chow diet. Intestines were harvested from 18-day-old fetuses and 1-, 3-, and 6-week-old mice (*n* = 5 or 6 per group for 1-, 3-, and 6-week-old mice; for fetus, *n* = 3 pooled intestinal samples of 3 individual intestines). For the mouse studies, both male and female mice were studied. No sexual dimorphism was observed in the vitamin D target genes at these ages.

To determine whether classical as well as novel responses to 1,25(OH)<sub>2</sub>D<sub>3</sub> occur in both villus and crypt, intestinal epithelial cells were isolated from both crypts and villi. The duodena from 3-month-old mice were washed in cold phosphate-buffered saline (PBS), cut into 1-cm pieces, and rotated in 3 mM EDTA in PBS at 4°C. After vigorous shaking to release the epithelium, crypts were depleted of contaminating villi by passing through a 70-μm cell strainer (BD Falcon, Tewksbury, MA). Villus epithelium was collected from the top of the 70-μm cell strainer (76). To test whether VDR target genes are conserved in humans, human enteroid cultures were used with either a crypt-like phenotype (i.e., high proliferation, undifferentiated cells) or a villus-like phenotype (i.e., low proliferation, differentiated cells). Human intestinal tissue specimens were obtained from endoscopy biopsies performed at Baylor College of

Medicine (BCM) from adult patients of both sexes (3 female and 3 male; before endoscopy biopsies, informed consent was obtained from the patients, and the Institutional Review Board at BCM approved this study). Crypts were isolated using the EDTA chelation method described above. For human enteroids, crypts were resuspended in Matrigel and plated in a 24-well plate. Enteroids were maintained in complete medium with growth factors (CMGF+) with medium changes every 2 to 3 days (77). Enteroids were split every week by passing them through an insulin syringe and replated in Matrigel. For treatment of enteroids with 1,25(OH)<sub>2</sub>D<sub>3</sub> or vehicle, enteroids were maintained in high-Wnt3A (undifferentiated) medium (CMGF+) or differentiation medium (CMGF+ without Wnt3A, nicotinamide, SB202, and R-Spondin) 3 days before treatment, with one medium change between (77). Subsequently, enteroids were treated with 100 nM 1,25(OH)<sub>2</sub>D<sub>3</sub> (Cayman Chemical Company) or vehicle (ethanol) at equal volumes in medium. Twenty-four hours following treatment, enteroids were collected and processed.

**RNA isolation and expression analysis.** Total RNA was isolated from mouse tissues, isolated mouse villus and crypt epithelia, and human organoids using RiboZol RNA extraction reagent (Amresco, Solon, OH) or TRIzol reagent (Invitrogen, Carlsbad, CA) according to the manufacturer's instructions and subsequently purified with an RNeasy Plus universal kit (Qiagen, Hilden, Germany) using on-column DNase digestion (Qiagen). RNA concentration was measured with a NanoDrop spectrophotometer (ND-1000; Isogen Life Science, Utrecht, The Netherlands). RNA integrity was assessed using a denaturing agarose gel stained with ethidium bromide (EtBr) or by using a bioanalyzer nanochip (Agilent Technologies, Santa Clara, CA). For quantitative real-time PCR (qRT-PCR), 2 μg of total RNA was used to synthesize cDNA using a Superscript III first-strand synthesis system (Invitrogen) according to the manufacturer's instructions. Relative quantification of target gene expression was performed using TaqMan analyses. TaqMan gene expression probes (Applied Biosystems, Foster City, CA) used for qRT-PCR were the following: *Cyp24a1* (Mm00487244-m1), *S100g* (Mm00486654-m1), *Slc30a1* (Mm00437377-m1), *Slc30a10* (Mm00437377-m1), *Slc37a2* (Mm00451435-m1), *Trpv5* (Mm01166037-m1), *Trpv6* (Mm00499069-m1), and *Tjp1* (ZO-1 gene; Mm01320638-m1). Reactions were performed in a 7500 real-time PCR system (Applied Biosystems). The cycle steps were as follows: an initial 3-min incubation at 95°C, followed by 40 cycles of 95°C for 10 s, 60°C for 30 s, and 72°C for 30 s. Expression levels of genes of interest were normalized to *Gapdh* (Mm999999-g1). The comparative threshold cycle ( $2^{-\Delta\Delta CT}$ ) method was used to calculate relative gene expression.

For global assessment of mouse RNA levels, total RNA was subjected to two rounds of poly(A) selection using oligo(dT)<sub>25</sub> magnetic beads (New England Biolabs [NEB], Ipswich, MA). Illumina-compatible RNA-seq libraries were constructed using the NEBNext Ultra II RNA library prep with sample purification beads (catalog number no. E7775) and NEBNext Multiplex Oligos for Illumina (dual index primers set 1; catalog no. E7600) according to the manufacturer's instructions. Poly(A) selection and library quality were assessed using TapeStation 2200 (Agilent Technologies, Santa Clara, CA), and libraries were quantified using Qubit 4.0 fluorometer (Thermo Fisher, Waltham, MA). The prepared libraries were sequenced on an Illumina NextSeq 500 instrument (Illumina, San Diego, CA). CLC Genomics Workbench version 11.0.1 (Qiagen, Venlo, Netherlands) was used for RNA-seq analysis. Demultiplexed fastq files from RNA-seq libraries were imported into the CLC software. Bases with low quality were trimmed, and reads were aligned to the *Mus musculus* reference genome build 9 (mm9) using Kallisto. The aligned reads were obtained using the RNA-seq analysis tool CLC Genomics Workbench. Kallisto (version 45) was utilized to quantify the transcript abundances of the RNA-seq samples through pseudoalignment, using single-end reads and an Ensembl mm9 transcriptome build index. The tximport (version 1.14.0) package (78) was run in R (version 3.6.2) to create gene level count matrices for use with DESeq2 (version 1.26) (79) by importing quantification data obtained from Kallisto. DESeq2 was then used to generate transcript levels in each tissue sample.

For global assessment of RNA levels from human enteroids samples, RNA-seq data were aligned to the reference human genome (hg38) using Kallisto. Subsequently, differential gene expressions for both mouse and human were assessed using DESeq2 in R, and transcript levels were obtained using a false-discovery rate of 0.05 and a cutoff 1.5-fold change.

For GO term analyses, transcript identifiers (IDs) were used with the biomaRt package (version 2.42) (80) along with RDavidWebService package (version 1.24) (81) as well as DAVID 6.8 (82) to identify biological processes, cellular components, and molecular functions in which input genes are enriched.

**Western blot analysis.** For Western blot analysis of VDR, total cellular protein was extracted with a lysis buffer containing 50 mM Tris-HCl (pH 7.5), 150 mM NaCl, 0.1% sodium dodecyl sulfate, 1.0% NP-40, and protease inhibitors. Protein content was measured using the Bradford assay (83) or a reducing agent- and detergent-compatible protein assay (Bio-Rad Laboratories, Inc., Hercules, CA). Fifty micrograms of denatured protein was subjected to sodium dodecyl sulfate-polyacrylamide gel electrophoresis (4% to 20% gradient gel; Bio-Rad Laboratories, Inc., Hercules, CA) and transferred to a polyvinylidene difluoride membrane (Bio-Rad Laboratories, Inc.) for Western blot analysis using an enhanced chemiluminescent detection system (Denville Scientific, Inc., Holliston, MA). β-Actin immunoblotting was used for sample normalization. Anti-VDR (D-6) (research resource identified [RRID], AB\_628040) and anti-β-actin (RRID, AB\_626632) as well as secondary antibodies were obtained from Santa Cruz Biotechnology, Inc. (Dallas, TX).

**Bone analysis.** μCT analysis of the left tibiae was performed *ex vivo* using a high-resolution SkyScan 1172 system (50 kV, 200 μA, 0.5-mm aluminum filter) to examine trabecular and cortical bone parameters (84). Serial tomographs, reconstructed from raw data using the cone-beam reconstruction software (NRecon, v.1.4.4.0; Skyscan), were used to compute trabecular and cortical parameters from the proximal metaphyseal and middiaphyseal areas, respectively. Analysis was performed according to the guidelines of the American Society for Bone and Mineral Research (85).



**Serum analysis.** Serum calcium, assayed using a colorimetric assay (Pointe Scientific, Inc., Canton, MI), was determined by Heartland Laboratories, Ames, IA.

**Statistical analysis.** Results are displayed as means  $\pm$  standard errors of the means (SEMs). Data were analyzed using Student's *t* test or analysis of variance (ANOVA) and additionally with Benjamini and Hochberg in a *post hoc* test to consider significant difference between groups ( $P < 0.05$ ).

**Data availability.** RNA-seq data from mouse tissues (GSE144978) and human enteroids (GSE159811) were deposited in the Gene Expression Omnibus of the National Center for Biotechnology.

## ACKNOWLEDGMENTS

We thank M. Aburadi and A. Kyeremateng for assistance with certain aspects of this investigation.

S.L., S.C., S.M., N.F.S., M.P.V., and J.C.F. designed the study. S.L., J.D.L.C., S. Hutchens, Z.K.C., R.A., O.P.-C., J.H., P.D., and L.V. performed experiments. S.L., S.C., S.M., N.F.S., Z.K.C., M.P.V., J.C.F., G.C., L.V., P.D., P.S., and S. Husain provided interpretation of results. S.L. and S.C. wrote the paper with comments from all authors.

This study was supported by NIH grant DK112365 (to S.C., M.P.V., J.C.F., and N.F.S.) and NIH grant ESO24812 to S.M. as well as a grant from the FWO:G0A2416N to L.V. and G.C.

We disclose no conflicts of interest.

## REFERENCES

- Christakos S, Dhawan P, Verstuyf A, Verlinden L, Carmeliet G. 2016. Vitamin D: metabolism, molecular mechanism of action, and pleiotropic effects. *Physiol Rev* 96:365–408. <https://doi.org/10.1152/physrev.00014.2015>.
- Pike JW, Meyer MB, Benkusky NA, Lee SM, St John H, Carlson A, Onal M, Shamsuzzaman S. 2016. Genomic determinants of vitamin D-regulated gene expression. *Vitam Horm* 100:21–44. <https://doi.org/10.1016/bs.vh.2015.10.011>.
- Pike JW, Christakos S. 2017. Biology and mechanisms of action of the vitamin D hormone. *Endocrinol Metab Clin North Am* 46:815–843. <https://doi.org/10.1016/j.ecl.2017.07.001>.
- Christakos S, Lieben L, Masuyama R, Carmeliet G. 2014. Vitamin D endocrine system and the intestine. *Bonekey Rep* 3:496. <https://doi.org/10.1038/bonekey.2013.230>.
- Christakos S. 2012. Recent advances in our understanding of 1,25-dihydroxyvitamin D<sub>3</sub> regulation of intestinal calcium absorption. *Arch Biochem Biophys* 523:73–76. <https://doi.org/10.1016/j.abb.2011.12.020>.
- Fujita H, Sugimoto K, Inatomi S, Maeda T, Osanai M, Uchiyama Y, Yamamoto Y, Wada T, Kojima T, Yokozaki H, Yamashita T, Kato S, Sawada N, Chiba H. 2008. Tight junction proteins claudin-2 and -12 are critical for vitamin D-dependent Ca<sup>2+</sup> absorption between enterocytes. *Mol Biol Cell* 19:1912–1921. <https://doi.org/10.1091/mbc.e07-09-0973>.
- Kutuzova GD, DeLuca HF. 2004. Gene expression profiles in rat intestine identify pathways for 1,25-dihydroxyvitamin D<sub>3</sub> stimulated calcium absorption and clarify its immunomodulatory properties. *Arch Biochem Biophys* 432:152–166. <https://doi.org/10.1016/j.abb.2004.09.004>.
- Wasserman RH, Fullmer CS. 1995. Vitamin D and intestinal calcium transport: facts, speculations and hypotheses. *J Nutr* 125:1971S–1979S. [https://doi.org/10.1093/jn/125.suppl\\_7.1971S](https://doi.org/10.1093/jn/125.suppl_7.1971S).
- Pansu D, Bellaton C, Roche C, Bronner F. 1983. Duodenal and ileal calcium absorption in the rat and effects of vitamin D. *Am J Physiol* 244:G695–700. <https://doi.org/10.1152/ajpgi.1983.244.6.G695>.
- Lee DB, Hu MS, Kayne LH, Nakhoul F, Jamgotchian N. 1991. The importance of non-vitamin D-mediated calcium absorption. *Contrib Nephrol* 91:14–20. <https://doi.org/10.1159/000420152>.
- Lee DB, Walling MM, Levine BS, Gafter U, Silis V, Hodsman A, Coburn JW. 1981. Intestinal and metabolic effect of 1,25-dihydroxyvitamin D<sub>3</sub> in normal adult rat. *Am J Physiol* 240:G90–G96. <https://doi.org/10.1152/ajpgi.1981.240.1.G90>.
- Favus MJ, Kathpalia SC, Coe FL, Mond AE. 1980. Effects of diet calcium and 1,25-dihydroxyvitamin D<sub>3</sub> on colon calcium active transport. *Am J Physiol* 238:G75–G78. <https://doi.org/10.1152/ajpgi.1980.238.2.G75>.
- Auchere D, Tardivel S, Gounelle JC, Druke T, Lacour B. 1998. Role of transcellular pathway in ileal Ca<sup>2+</sup> absorption: stimulation by low-Ca<sup>2+</sup> diet. *Am J Physiol* 275:G951–G956.
- Dhawan P, Veldurthy V, Yehia G, Hsaio C, Porta A, Kim KI, Patel N, Lieben L, Verlinden L, Carmeliet G, Christakos S. 2017. Transgenic expression of the vitamin D receptor restricted to the ileum, cecum, and colon of vitamin D receptor knockout mice rescues vitamin D receptor-dependent rickets. *Endocrinology* 158:3792–3804. <https://doi.org/10.1210/en.2017-00258>.
- Kong J, Zhang Z, Musch MW, Ning G, Sun J, Hart J, Bissonnette M, Li YC. 2008. Novel role of the vitamin D receptor in maintaining the integrity of the intestinal mucosal barrier. *Am J Physiol Gastrointest Liver Physiol* 294:G208–G216. <https://doi.org/10.1152/ajpgi.00398.2007>.
- Sun J. 2010. Vitamin D and mucosal immune function. *Curr Opin Gastroenterol* 26:591–595. <https://doi.org/10.1097/MOG.0b013e32833d4b9f>.
- Barbachano A, Fernandez-Barral A, Ferrer-Mayorga G, Costales-Carrera A, Larriba MJ, Munoz A. 2017. The endocrine vitamin D system in the gut. *Mol Cell Endocrinol* 453:79–87. <https://doi.org/10.1016/j.mce.2016.11.028>.
- Lee SM, Riley EM, Meyer MB, Benkusky NA, Plum LA, DeLuca HF, Pike JW. 2015. 1,25-Dihydroxyvitamin D<sub>3</sub> controls a cohort of vitamin D receptor target genes in the proximal intestine that is enriched for calcium-regulating components. *J Biol Chem* 290:18199–18215. <https://doi.org/10.1074/jbc.M115.665794>.
- Claro da Silva T, Hiller C, Gai Z, Kullak-Ublick GA. 2016. Vitamin D<sub>3</sub> transactivates the zinc and manganese transporter SLC30A10 via the vitamin D receptor. *J Steroid Biochem Mol Biol* 163:77–87. <https://doi.org/10.1016/j.jsbmb.2016.04.006>.
- Reynolds CJ, Koszewski NJ, Horst RL, Beitz DC, Goff JP. 2019. Localization of the 1,25-dihydroxyvitamin D-mediated response in the intestines of mice. *J Steroid Biochem Mol Biol* 186:56–60. <https://doi.org/10.1016/j.jsbmb.2018.09.009>.
- Colston KW, Mackay AG, Finlayson C, Wu JC, Maxwell JD. 1994. Localization of vitamin D receptor in normal human duodenum and in patients with coeliac disease. *Gut* 35:1219–1225. <https://doi.org/10.1136/gut.35.9.1219>.
- Peregrina K, Houston M, Daroqui C, Dhima E, Sellers RS, Augenlicht LH. 2015. Vitamin D is a determinant of mouse intestinal Lgr5 stem cell functions. *Carcinogenesis* 36:25–31. <https://doi.org/10.1093/carcin/bgu221>.
- Mukhopadhyay S. 2018. Familial manganese-induced neurotoxicity due to mutations in SLC30A10 or SLC39A14. *Neurotoxicology* 64:278–283. <https://doi.org/10.1016/j.neuro.2017.07.030>.
- Kellett GL. 2011. Alternative perspective on intestinal calcium absorption: proposed complementary actions of Ca(v)1.3 and TRPV6. *Nutr Rev* 69:347–370. <https://doi.org/10.1111/j.1753-4887.2011.00395.x>.
- Mittermeier L, Demirkhanyan L, Stadlbauer B, Breit A, Recordati C, Hilgen-dorff A, Matsushita M, Braun A, Simmons DG, Zakharian E, Gudermann T, Chubanov V. 2019. TRPM7 is the central gatekeeper of intestinal mineral absorption essential for postnatal survival. *Proc Natl Acad Sci U S A* 116:4706–4715. <https://doi.org/10.1073/pnas.1810633116>.
- Halloran BP, DeLuca HF. 1980. Calcium transport in small intestine

- during early development: role of vitamin D. *Am J Physiol* 239: G473–G479. <https://doi.org/10.1152/ajpgi.1980.239.6.G473>.
27. Hutchens S, Liu C, Jursa T, Shawlot W, Chaffee BK, Yin W, Gore AC, Aschner M, Smith DR, Mukhopadhyay S. 2017. Deficiency in the manganese efflux transporter SLC30A10 induces severe hypothyroidism in mice. *J Biol Chem* 292:9760–9773. <https://doi.org/10.1074/jbc.M117.783605>.
  28. Zhang YG, Wu S, Sun J. 2013. Vitamin D, vitamin D receptor, and tissue barriers. *Tissue Barriers* 1:e23118. <https://doi.org/10.4161/tisb.23118>.
  29. Jiang H, Horst RL, Koszewski NJ, Goff JP, Christakos S, Fleet JC. 2020. Targeting 1,25(OH)<sub>2</sub>D-mediated calcium absorption machinery in proximal colon with calcitriol glycosides and glucuronides. *J Steroid Biochem Mol Biol* 198:105574. <https://doi.org/10.1016/j.jsbmb.2019.105574>.
  30. Stumpf WE, Sar M, Reid FA, Tanaka Y, DeLuca HF. 1979. Target cells for 1,25-dihydroxyvitamin D<sub>3</sub> in intestinal tract, stomach, kidney, skin, pituitary, and parathyroid. *Science* 206:1188–1190. <https://doi.org/10.1126/science.505004>.
  31. Stumpf WE. 2008. Vitamin D and the digestive system. *Eur J Drug Metab Pharmacokin* 33:85–100. <https://doi.org/10.1007/BF03191025>.
  32. Wang Y, Zhu J, DeLuca HF. 2012. Where is the vitamin D receptor? *Arch Biochem Biophys* 523:123–133. <https://doi.org/10.1016/j.abb.2012.04.001>.
  33. Fernandez-Barral A, Costales-Carrera A, Buira SP, Jung P, Ferrer-Mayorga G, Larriba MJ, Bustamante-Madrid P, Dominguez O, Real FX, Guerra-Pastrian L, Lafarga M, Garcia-Olmo D, Cantero R, Del Peso L, Battle E, Rojo F, Munoz A, Barbachano A. 2020. Vitamin D differentially regulates colon stem cells in patient-derived normal and tumor organoids. *FEBS J* 287: 53–72. <https://doi.org/10.1111/febs.14998>.
  34. Li W, Peregrina K, Houston M, Augenlicht LH. 2020. Vitamin D and the nutritional environment in functions of intestinal stem cells: implications for tumorigenesis and prevention. *J Steroid Biochem Mol Biol* 198: 105556. <https://doi.org/10.1016/j.jsbmb.2019.105556>.
  35. Wu JC, Smith MW, Lawson DE. 1992. Time dependency of 1,25(OH)<sub>2</sub>D<sub>3</sub> induction of calbindin mRNA and calbindin expression in chick enterocytes during their differentiation along the crypt-villus axis. *Differentiation* 51:195–200. <https://doi.org/10.1111/j.1432-0436.1992.tb00696.x>.
  36. Meyer MB, Watanuki M, Kim S, Shevde NK, Pike JW. 2006. The human transient receptor potential vanilloid type 6 distal promoter contains multiple vitamin D receptor binding sites that mediate activation by 1,25-dihydroxyvitamin D<sub>3</sub> in intestinal cells. *Mol Endocrinol* 20: 1447–1461. <https://doi.org/10.1210/me.2006-0031>.
  37. Wood RJ, Tchack L, Taparia S. 2001. 1,25-Dihydroxyvitamin D<sub>3</sub> increases the expression of the CaT1 epithelial calcium channel in the Caco-2 human intestinal cell line. *BMC Physiol* 1:11. <https://doi.org/10.1186/1472-6793-1-11>.
  38. Fleet JC, Eksir F, Hance KW, Wood RJ. 2002. Vitamin D-inducible calcium transport and gene expression in three Caco-2 cell lines. *Am J Physiol Gastrointest Liver Physiol* 283:G618–G625. <https://doi.org/10.1152/ajpgi.00269.2001>.
  39. Walters JR, Balesaria S, Chavele KM, Taylor V, Berry JL, Khair U, Barley NF, van Heel DA, Field J, Hayat JO, Bhattacharjee A, Jeffery R, Poulosom R. 2006. Calcium channel TRPV6 expression in human duodenum: different relationships to the vitamin D system and aging in men and women. *J Bone Miner Res* 21:1770–1777. <https://doi.org/10.1359/jbmr.060721>.
  40. Balesaria S, Sangha S, Walters JR. 2009. Human duodenum responses to vitamin D metabolites of TRPV6 and other genes involved in calcium absorption. *Am J Physiol Gastrointest Liver Physiol* 297:G1193–G1197. <https://doi.org/10.1152/ajpgi.00237.2009>.
  41. Taylor CA, Hutchens S, Liu C, Jursa T, Shawlot W, Aschner M, Smith DR, Mukhopadhyay S. 2019. SLC30A10 transporter in the digestive system regulates brain manganese under basal conditions while brain SLC30A10 protects against neurotoxicity. *J Biol Chem* 294:1860–1876. <https://doi.org/10.1074/jbc.RA118.005628>.
  42. Leyva-Illades D, Chen P, Zogzas CE, Hutchens S, Mercado JM, Swaim CD, Morrisett RA, Bowman AB, Aschner M, Mukhopadhyay S. 2014. SLC30A10 is a cell surface-localized manganese efflux transporter, and parkinsonism-causing mutations block its intracellular trafficking and efflux activity. *J Neurosci* 34:14079–14095. <https://doi.org/10.1523/JNEUROSCI.2329-14.2014>.
  43. Tuschl K, Clayton PT, Gospe SM, Jr, Gulab S, Ibrahim S, Singhi P, Aulakh R, Ribeiro RT, Barsottini OG, Zaki MS, Del Rosario ML, Dyack S, Price V, Rideout A, Gordon K, Wevers RA, Chong WK, Mills PB. 2012. Syndrome of hepatic cirrhosis, dystonia, polycythemia, and hypermanganesemia caused by mutations in SLC30A10, a manganese transporter in man. *Am J Hum Genet* 90:457–466. <https://doi.org/10.1016/j.ajhg.2012.01.018>.
  44. Quadri M, Federico A, Zhao T, Breedveld GJ, Battisti C, Delnooz C, Severijnen LA, Di Toro Mammarella L, Mignarri A, Monti L, Sanna A, Lu P, Punzo F, Cossu G, Willemsen R, Rasi F, Oostra BA, van de Warrenburg BP, Bonifati V. 2012. Mutations in SLC30A10 cause parkinsonism and dystonia with hypermanganesemia, polycythemia, and chronic liver disease. *Am J Hum Genet* 90:467–477. <https://doi.org/10.1016/j.ajhg.2012.01.017>.
  45. Mercadante CJ, Prajapati M, Conboy HL, Dash ME, Herrera C, Pettiglio MA, Cintron-Rivera L, Salesky MA, Rao DB, Bartnikas TB. 2019. Manganese transporter SLC30A10 controls physiological manganese excretion and toxicity. *J Clin Invest* 129:5442–5461. <https://doi.org/10.1172/JCI129710>.
  46. Chen P, Bornhorst J, Aschner M. 2018. Manganese metabolism in humans. *Front Biosci (Landmark Ed)* 23:1655–1679. <https://doi.org/10.2741/4665>.
  47. Rico H, Gomez-Raso N, Revilla M, Hernandez ER, Seco C, Paez E, Crespo E. 2000. Effects on bone loss of manganese alone or with copper supplement in ovariectomized rats. *Eur J Obstet Gynecol Reprod Biol* 90:97–101. [https://doi.org/10.1016/S0301-2115\(99\)00223-7](https://doi.org/10.1016/S0301-2115(99)00223-7).
  48. Heaney RP. 1988. Nutritional factors in causation of osteoporosis. *Ann Chir Gynaecol* 77:176–179.
  49. Hreha J, Wey A, Cunningham C, Krell ES, Brietbart EA, Paglia DN, Montemurro NJ, Nguyen DA, Lee YJ, Komlos D, Lim E, Benevenia J, O'Connor JP, Lin SS. 2015. Local manganese chloride treatment accelerates fracture healing in a rat model. *J Orthop Res* 33:122–130. <https://doi.org/10.1002/jor.22733>.
  50. Liu C, Hutchens S, Jursa T, Shawlot W, Polishchuk EV, Polishchuk RS, Dray BK, Gore AC, Aschner M, Smith DR, Mukhopadhyay S. 2017. Hypothyroidism induced by loss of the manganese efflux transporter SLC30A10 may be explained by reduced thyroxine production. *J Biol Chem* 292: 16605–16615. <https://doi.org/10.1074/jbc.M117.804989>.
  51. Anagianni S, Tuschl K. 2019. Genetic disorders of manganese metabolism. *Curr Neurol Neurosci Rep* 19:33. <https://doi.org/10.1007/s11910-019-0942-y>.
  52. Song Y, Peng X, Porta A, Takanaga H, Peng JB, Hediger MA, Fleet JC, Christakos S. 2003. Calcium transporter 1 and epithelial calcium channel messenger ribonucleic acid are differentially regulated by 1,25 dihydroxyvitamin D<sub>3</sub> in the intestine and kidney of mice. *Endocrinology* 144:3885–3894. <https://doi.org/10.1210/en.2003-0314>.
  53. Huet T, Laverny G, Ciesielski F, Molnar F, Ramamoorthy TG, Belorusova AY, Antony P, Potier N, Metzger D, Moras D, Rochel N. 2015. A vitamin D receptor selectively activated by gemini analogs reveals ligand dependent and independent effects. *Cell Rep* 10:516–526. <https://doi.org/10.1016/j.celrep.2014.12.045>.
  54. Lee SM, Pike JW. 2016. The vitamin D receptor functions as a transcription regulator in the absence of 1,25-dihydroxyvitamin D<sub>3</sub>. *J Steroid Biochem Mol Biol* 164:265–270. <https://doi.org/10.1016/j.jsbmb.2015.08.018>.
  55. Bertinchamps AJ, Miller ST, Cotzias GC. 1966. Interdependence of routes excreting manganese. *Am J Physiol* 211:217–224. <https://doi.org/10.1152/ajplegacy.1966.211.1.217>.
  56. Kovacs G, Danko T, Bergeron MJ, Balazs B, Suzuki Y, Zsembery A, Hediger MA. 2011. Heavy metal cations permeate the TRPV6 epithelial cation channel. *Cell Calcium* 49:43–55. <https://doi.org/10.1016/j.ceca.2010.11.007>.
  57. Fasolato C, Hoth M, Matthews G, Penner R. 1993. Ca<sup>2+</sup> and Mn<sup>2+</sup> influx through receptor-mediated activation of nonspecific cation channels in mast cells. *Proc Natl Acad Sci U S A* 90:3068–3072. <https://doi.org/10.1073/pnas.90.7.3068>.
  58. Gavin CE, Gunter KK, Gunter TE. 1999. Manganese and calcium transport in mitochondria: implications for manganese toxicity. *Neurotoxicology* 20:445–453.
  59. Kamer KJ, Sancak Y, Fomina Y, Meisel JD, Chaudhuri D, Grabarek Z, Mootha VK. 2018. MICU1 imparts the mitochondrial uniporter with the ability to discriminate between Ca<sup>2+</sup> and Mn<sup>2+</sup>. *Proc Natl Acad Sci U S A* 115:E7960–E7969. <https://doi.org/10.1073/pnas.1807811115>.
  60. Vinogradov A, Scarpa A. 1973. The initial velocities of calcium uptake by rat liver mitochondria. *J Biol Chem* 248:5527–5531.
  61. Ijomone OM, Aluko OM, Okoh COA, Martins AC, Jr, Aschner M. 2019. Role for calcium signaling in manganese neurotoxicity. *J Trace Elem Med Biol* 56:146–155. <https://doi.org/10.1016/j.jtemb.2019.08.006>.
  62. Bornhorst J, Wehe CA, Huwel S, Karst U, Galla HJ, Schwerdtle T. 2012. Impact of manganese on and transfer across blood-brain and blood-

- cerebrospinal fluid barrier *in vitro*. *J Biol Chem* 287:17140–17151. <https://doi.org/10.1074/jbc.M112.344093>.
63. Levy M, Elkoshi N, Barber-Zucker S, Hoch E, Zarivach R, Hershinkel M, Sekler I. 2019. Zinc transporter 10 (ZnT10)-dependent extrusion of cellular Mn<sup>2+</sup> is driven by an active Ca<sup>2+</sup>-coupled exchange. *J Biol Chem* 294:5879–5889. <https://doi.org/10.1074/jbc.RA118.006816>.
  64. Wilfinger J, Seuter S, Tuomainen TP, Virtanen JK, Voutilainen S, Nurmi T, de Mello VD, Uusitupa M, Carlberg C. 2014. Primary vitamin D receptor target genes as biomarkers for the vitamin D<sub>3</sub> status in the hematopoietic system. *J Nutr Biochem* 25:875–884. <https://doi.org/10.1016/j.jnutbio.2014.04.002>.
  65. Pan CJ, Chen SY, Jun HS, Lin SR, Mansfield BC, Chou JY. 2011. SLC37A1 and SLC37A2 are phosphate-linked, glucose-6-phosphate antiporters. *PLoS One* 6:e23157. <https://doi.org/10.1371/journal.pone.0023157>.
  66. Cousins RJ. 2010. Gastrointestinal factors influencing zinc absorption and homeostasis. *Int J Vitam Nutr Res* 80:243–248. <https://doi.org/10.1024/0300-9831/a000030>.
  67. Rossi L, Migliaccio S, Corsi A, Marzia M, Bianco P, Teti A, Gambelli L, Cianfarani S, Paoletti F, Branca F. 2001. Reduced growth and skeletal changes in zinc-deficient growing rats are due to impaired growth plate activity and inanition. *J Nutr* 131:1142–1146. <https://doi.org/10.1093/jn/131.4.1142>.
  68. Lieben L, Carmeliet G, Masuyama R. 2011. Calcemic actions of vitamin D: effects on the intestine, kidney and bone. *Best Pract Res Clin Endocrinol Metab* 25:561–572. <https://doi.org/10.1016/j.beem.2011.05.008>.
  69. Koo SI, Fullmer CS, Wasserman RH. 1980. Effect to cholecalciferol and 1,25-dihydroxycholecalciferol on the intestinal absorption of zinc in the chick. *J Nutr* 110:1813–1818. <https://doi.org/10.1093/jn/110.9.1813>.
  70. Williams KB, DeLuca HF. 2007. Characterization of intestinal phosphate absorption using a novel *in vivo* method. *Am J Physiol Endocrinol Metab* 292:E1917–E1921. <https://doi.org/10.1152/ajpendo.00654.2006>.
  71. Knopfel T, Pastor-Arroyo EM, Schnitzbauer U, Kratschmar DV, Odermatt A, Pellegrini G, Hernando N, Wagner CA. 2017. The intestinal phosphate transporter NaP<sub>i</sub>-IIb (Slc34a2) is required to protect bone during dietary phosphate restriction. *Sci Rep* 7:11018. <https://doi.org/10.1038/s41598-017-10390-2>.
  72. Marks J. 2019. The role of SLC34A2 in intestinal phosphate absorption and phosphate homeostasis. *Pflugers Arch* 471:165–173. <https://doi.org/10.1007/s00424-018-2221-1>.
  73. Katai K, Miyamoto K, Kishida S, Segawa H, Nii T, Tanaka H, Tani Y, Arai H, Tatsumi S, Morita K, Taketani Y, Takeda E. 1999. Regulation of intestinal Na<sup>+</sup>-dependent phosphate co-transporters by a low-phosphate diet and 1,25-dihydroxyvitamin D<sub>3</sub>. *Biochem J* 343 Pt 3:705–712. <https://doi.org/10.1042/0264-6021:3430705>.
  74. Capuano P, Radanovic T, Wagner CA, Bacic D, Kato S, Uchiyama Y, St-Arnaud R, Murer H, Biber J. 2005. Intestinal and renal adaptation to a low-P<sub>i</sub> diet of type II NaP<sub>i</sub> cotransporters in vitamin D receptor- and 1αOHase-deficient mice. *Am J Physiol Cell Physiol* 288:C429–C434. <https://doi.org/10.1152/ajpcell.00331.2004>.
  75. Hinoi T, Akyol A, Theisen BK, Ferguson DO, Greenson JK, Williams BO, Cho KR, Fearon ER. 2007. Mouse model of colonic adenoma-carcinoma progression based on somatic Apc inactivation. *Cancer Res* 67:9721–9730. <https://doi.org/10.1158/0008-5472.CAN-07-2735>.
  76. Chen L, Vasoya RP, Toke NH, Parthasarathy A, Luo S, Chiles E, Flores J, Gao N, Bonder EM, Su X, Verzi MP. 2020. HNF4 regulates fatty acid oxidation and is required for renewal of intestinal stem cells in mice. *Gastroenterology* 158:985.e9–999.e9. <https://doi.org/10.1053/j.gastro.2019.11.031>.
  77. Mahe MM, Sundaram N, Watson CL, Shroyer NF, Helmrath MA. 2015. Establishment of human epithelial enteroids and colonoids from whole tissue and biopsy. *J Vis Exp* 6:52483. <https://doi.org/10.3791/52483>.
  78. Sonesson C, Love MI, Robinson MD. 2015. Differential analyses for RNA-seq: transcript-level estimates improve gene-level inferences. *F1000Res* 4:1521. <https://doi.org/10.12688/f1000research.7563.1>.
  79. Love MI, Huber W, Anders S. 2014. Moderated estimation of fold change and dispersion for RNA-seq data with DESeq2. *Genome Biol* 15:550. <https://doi.org/10.1186/s13059-014-0550-8>.
  80. Durinck S, Spellman PT, Birney E, Huber W. 2009. Mapping identifiers for the integration of genomic datasets with the R/Bioconductor package biomaRt. *Nat Protoc* 4:1184–1191. <https://doi.org/10.1038/nprot.2009.97>.
  81. Fresno C, Fernandez EA. 2013. RDAVIDWebService: a versatile R interface to DAVID. *Bioinformatics* 29:2810–2811. <https://doi.org/10.1093/bioinformatics/btt487>.
  82. Huang da W, Sherman BT, Lempicki RA. 2009. Systematic and integrative analysis of large gene lists using DAVID bioinformatics resources. *Nat Protoc* 4:44–57. <https://doi.org/10.1038/nprot.2008.211>.
  83. Bradford MM. 1976. A rapid and sensitive method for the quantitation of microgram quantities of protein utilizing the principle of protein-dye binding. *Anal Biochem* 72:248–254. [https://doi.org/10.1016/0003-2697\(76\)90527-3](https://doi.org/10.1016/0003-2697(76)90527-3).
  84. Lieben L, Benn BS, Ajibade D, Stockmans I, Moermans K, Hediger MA, Peng JB, Christakos S, Bouillon R, Carmeliet G. 2010. Trpv6 mediates intestinal calcium absorption during calcium restriction and contributes to bone homeostasis. *Bone* 47:301–308. <https://doi.org/10.1016/j.bone.2010.04.595>.
  85. Bouxsein ML, Boyd SK, Christiansen BA, Guldberg RE, Jepsen KJ, Muller R. 2010. Guidelines for assessment of bone microstructure in rodents using micro-computed tomography. *J Bone Miner Res* 25:1468–1486. <https://doi.org/10.1002/jbmr.141>.